has been developed (37, 38, 66, 71). In this study, by using the virus infection system, we examined the possible effect of HCV infection on the fate of the host cell. We report here that HCV infection induces apoptosis via the mitochondrion-mediated pathway, as demonstrated by the increased accumulation of the proapoptotic protein Bax on the mitochondria, decreased mitochondrial transmembrane potential, and mitochondrial swelling, which result in the release of cytochrome *c* from the mitochondria and the activation of caspase 3.

## MATERIALS AND METHODS

**Cells.** The Huh7.5 cell line (6), a highly HCV-susceptible subclone of Huh7 cells, was a kind gift from C. M. Rice, Center for the Study of Hepatitis C, The Rockefeller University. The cells were propagated in Dulbecco's modified Eagle medium supplemented with 10% heat-inactivated fetal bovine serum and 0.1 mM nonessential amino acids.

**Virus.** The virus stock used in this study was prepared as described below. The pFL-J6/JFH1 plasmid, encoding the entire viral genome of a chimeric strain of HCV genotype 2a, J6/JFH1 (37), was kindly provided by C. M. Rice. The plasmid was linearized by XbaI digestion and in vitro transcribed by using T7 RiboMAX (Promega, Madison, WI) to generate the full-length viral genomic RNA. The in vitro-transcribed RNA (10 μg) was transfected into Huh7.5 cells by means of electroporation (975 μF, 270 V) using Gene Pulser (Bio-Rad, Hercules, CA). The cells were then cultured in complete medium, and the supernatant was propagated as an original virus (J6/JFH1-passage 1 [J6/JFH1-P1]). Since the infectious titer of the original virus was not high enough for infection of all the cells in the culture at once, an adapted strain of the virus was obtained by passaging the virus-infected cells 47 times. The adapted virus (J6/JFH1-P47), which is a pool of adapted mutants, possesses 10 amino acid mutations (K78E, T396A, T416A, N534H, A712V, Y852H, W879R, F2281L, M2876L, and T2925A) and a single nucleotide mutation in the 5′-untranslated region (U146A) and produces a much higher titer of infectivity in Huh7.5 cell cultures than the original J6/JFH1-P1 (our unpublished data). Virus infection was performed at a multiplicity of infection of 2.0. Culture supernatants of uninfected cells served as a control (mock preparation).

Virus infectivity was measured by indirect immunofluorescence analysis, as described below, and expressed as cell-infecting units/ml.

**Cell viability/proliferation assay.** Huh7.5 cells were seeded in 96-well plates at a density of $1.0 \times 10^4$ cells/well and cultured overnight. The cells were then infected with the virus or the mock preparation, and, at different time points, cell viability/proliferation was determined by the WST-1 assay (Roche, Mannheim, Germany), as described previously (43).

**Detection of apoptosis.** The degree of apoptosis was measured by using a Cell Death Detection ELISA$^{Plus}$ kit (Roche), which is based on the determination of cytoplasmic histone-associated DNA fragments, according to the manufacturer's protocol. In brief, cells cultured in a 96-well plate were centrifuged at $200 \times g$ for 10 min at 4°C to remove the supernatant. After the cells were lysed with lysis buffer, the plate was centrifuged at $200 \times g$ for 10 min to separate the cytoplasmic and nuclear fractions. Twenty microliters of supernatant was placed in each well of a streptavidin-coated 96-well plate. Subsequently, a mixture of biotin-labeled anti-histone antibody and peroxidase-labeled anti-DNA antibody was added and wells were incubated for 2 h at room temperature. After wells were washed three times to remove the unbound components, peroxidase activities were determined photometrically with 2,2′-azino-diethyl-benzthiazolin sulfonate as a substrate and measured by using a microplate reader (Bio-Rad).

**Caspase enzymatic activities.** Activities of caspase 3, 8, and 9 were measured by using Caspase-Glo 3/7, 8, and 9 assays (Promega), respectively, according to the manufacturer's instructions. In brief, a proluminescence caspase 3/7, 8, or 9 substrate, which consists of aminoluciferin (substrate for luciferase) and the tetrapeptide sequence DEVD, LETD, or LEHD (cleavage site for caspase 3/7, 8, or 9, respectively), was added to cultured cells in each well of a 96-well plate, and the plate was incubated for 30 min at room temperature. In the presence of caspase 3/7, 8, or 9, aminoluciferin was liberated from the proluminescence substance and utilized as a substrate for the luciferase reaction. The resultant luminescence in relative light units was measured by using a Luminescencer-JNR AB-2100 (Atto, Tokyo, Japan).

**Cell fractionation.** Cells were fractionated by using a mitochondrial isolation kit (Pierce, Rockford, IL), according to the manufacturer's instructions. Briefly, $2 \times 10^7$ cells were harvested and suspended in reagent A containing a protease inhibitor cocktail (Roche). The cell suspension was mixed with buffer B, vortexed for 5 min, and then mixed with reagent C. The nuclei and unbroken cells were removed by centrifugation at $700 \times g$ for 10 min at 4°C, and the supernatant was used as cell lysate. The cell lysate was further centrifuged at $3,000 \times g$ for 15 min at 4°C. The pellet obtained, which was considered the mitochondrial fraction, was washed once with reagent C and dissolved in a lysis buffer containing 10 mM Tris-HCl (pH 7.5), 150 mM NaCl, 1 mM EDTA, 1% NP-40, and a protease inhibitor cocktail. The remaining supernatant was further centrifuged at $100,000 \times g$ for 30 min at 4°C, and the resultant supernatant was collected as a cytosolic fraction.

To verify successful mitochondrial fractionation, the cytosolic and mitochondrial fractions were analyzed by immunoblotting, as described below, using antibody against Tim23, a mitochondrion-specific protein.

**Analysis of the mitochondrial transmembrane potential.** The mitochondrial transmembrane potential was measured by flow cytometry using the cationic lipophilic green fluorochrome rhodamine 123 (Rho123; Sigma, St. Louis, MO), as described previously (43). Briefly, cells ($7 \times 10^5$) were harvested, washed twice with phosphate-buffered saline (PBS), and incubated with Rho123 (0.5 μg/ml) at 37°C for 25 min. The cells were then washed twice with PBS, and Rho123 intensity was analyzed by a flow cytometer (Becton Dickinson, San Jose, CA). A total of 10,000 events were collected per sample. Mean fluorescence intensities were measured by calculating the geometric mean for each histogram peak.

**Detection of morphological changes of the mitochondria.** Mitochondrial morphology was analyzed by two different methods. (i) For fluorescence microscopy, Huh7.5 cells seeded on glass coverslips in a 24-well plate were incubated for 30 min at 37°C with 100 nM MitoTracker (Molecular Probes, Eugene, OR). After being washed twice with PBS, the cells were fixed with 3.7% paraformaldehyde and observed under a confocal laser scanning microscope (Carl Zeiss, Oberkochen, Germany). When needed, the fixed cells were subjected to indirect immunofluorescence to confirm HCV infection, as described below. (ii) Electron microscopy was performed as described previously (23, 43). In brief, cells were fixed with 4% paraformaldehyde and 0.2% glutaraldehyde for 30 min at room temperature. After being washed with PBS, the cells were collected, dehydrated in a series of 70%, 80%, and 90% ethanol, embedded in LR White resin (London Resin, Berkshire, United Kingdom), and kept at −20°C for 2 days to facilitate resin polymerization. After ultrathin sectioning, samples were etched in 3% $H_2O_2$ for 5 min at room temperature and washed with PBS. Sections were stained with uranyl acetate and lead citrate and observed under a transmission electron microscope (JEM 1299EX; JOEL, Tokyo, Japan).

**Detection of mitochondrial superoxide.** Cells seeded on glass coverslips in a 24-well plate were incubated with 5 μM MitoSOX Red (Molecular Probes) at 37°C for 10 min. After being washed with warm Hanks' balanced salt solution with calcium and magnesium (Invitrogen, Carlsbad, CA), the cells were fixed with 3.7% paraformaldehyde and observed under a confocal laser scanning microscope (Carl Zeiss). When needed, the fixed cells were subjected to indirect immunofluorescence to confirm HCV infection, as described below.

**Indirect immunofluorescence.** Cells seeded on glass coverslips in a 24-well plate at a density of $6 \times 10^4$ cells/well were infected with HCV or left uninfected. At different time points after virus infection, the cells were fixed with 3.7% paraformaldehyde in PBS for 15 min at room temperature and permeabilized in 0.1% Triton X-100 in PBS for 15 min at room temperature. After being washed with PBS twice, cells were consecutively stained with primary and secondary antibodies. Primary antibodies used were anti-active caspase 3 rabbit polyclonal antibody (Promega) and an HCV-infected patient's serum. Secondary antibodies used were Cy3-conjugated donkey anti-rabbit immunoglobulin G (IgG; Chemicon, Temecula, CA), Alexa Fluor 594-conjugated goat anti-human IgG (Molecular Probes), and fluorescein isothiocyanate (FITC)-conjugated goat anti-human IgG (MBL, Nagoya, Japan). The cells were washed with PBS, counterstained with Hoechst 33342 solution (Molecular Probes) at room temperature for 10 min, mounted on glass slides, and observed under a confocal laser scanning microscope (Carl Zeiss). The specificity of this immunostaining was confirmed by using mouse monoclonal antibody against HCV core protein (C7-50; Abcam, Tokyo, Japan).

To analyze the possible localization of the activated Bax on mitochondrial membranes, cells were incubated with MitoTracker and subjected to immunofluorescence analysis using rabbit polyclonal antibody against activated Bax (NT antibody; Upstate, Lake Placid, NY). This antibody is directed toward N-terminal residues 1 to 21 of Bax in an N-terminal conformation-dependent manner and specifically recognizes the active form of Bax, in which this segment is exposed in response to apoptotic stimuli (64).

**Immunoblotting.** Cells were lysed in a buffer containing 10 mM Tris-HCl (pH 7.5), 150 mM NaCl, 1 mM EDTA, 1% NP-40, and a protease inhibitor cocktail (Roche). After two freeze-thaw cycles, cell debris was removed by

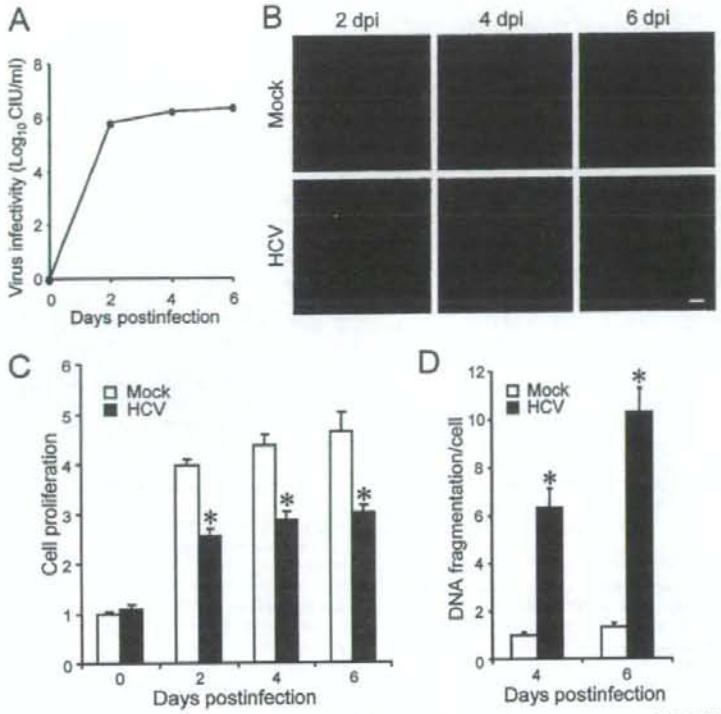


FIG. 1. HCV infection induces apoptosis in Huh7.5 cells. (A) Virus infectivity in the culture supernatants of HCV-infected cells. (B) Detection of HCV antigens in the cells. Huh7.5 cells mock inoculated or inoculated with HCV were subjected to indirect immunofluorescence analysis to detect HCV antigens (red staining) using an HCV-infected patient's serum and Alexa Fluor 594-conjugated goat anti-human IgG at 2, 4, and 6 days postinfection (dpi). Nuclei were counterstained with Hoechst 33342 (blue staining). Scale bar, 50 μm. (C) Cell viability/proliferation was measured for HCV-infected cultures and the mock-inoculated controls. Proliferation of the control cells at day 0 postinfection was arbitrarily expressed as 1.0. Data represent means ± standard deviations (SD) of three independent experiments. *, $P < 0.01$, compared with the control. (D) DNA fragmentation was measured as an index of apoptotic cell death for HCV-infected cultures and the mock-inoculated controls. DNA fragmentation of the control cells at 4 days postinfection was arbitrarily expressed as 1.0. Data represent means ± SD of three independent experiments. *, $P < 0.01$, compared with the control.

centrifugation. Protein quantification was carried out using a bicinchoninic acid protein assay kit (Pierce). Equal amounts of soluble proteins (4 to 20 μg) were subjected to sodium dodecyl sulfate-polyacrylamide gel electrophoresis and transferred onto a polyvinylidene difluoride membrane (Millipore, Bedford, MA), which was then incubated with the respective primary antibody. The primary antibodies used were mouse monoclonal antibodies against cytochrome *c* (A-8; Santa Cruz Biotechnology, Santa Cruz, CA), HCV NS3 (Chemicon), Tim23, Bax and Bcl-2 (BD Biosciences Pharmingen, San Diego, CA); rabbit polyclonal antibodies against Bak (Upstate), caspase 3, and PARP (Cell Signaling Technology, Danvers, MA); and goat polyclonal antibodies against glucose-regulated protein 78 (GRP78) and GRP94 (Santa Cruz Biotechnology). Horseradish peroxidase-conjugated goat anti-mouse IgG (MBL), goat anti-rabbit IgG (Bio-Rad), and donkey anti-goat IgG (Santa Cruz Biotechnology) were used as secondary antibodies. In some experiments, a commercial kit that facilitates the antigen-antibody reaction (Can Get Signal; Toyobo, Osaka, Japan) was used to obtain stronger signals. The respective protein bands were visualized by means of an enhanced chemiluminescence (GE Healthcare, Buckinghamshire, United Kingdom), and the intensity of each band was quantified by using NIH Image J. Protein loading was normalized by probing with goat antibody against actin (Santa Cruz Biotechnology) as a primary antibody.

**Statistical analysis.** The two-tailed Student *t* test was applied to evaluate the statistical significance of differences measured from the data sets. A *P* value of <0.05 was considered statistically significant.

## RESULTS

**HCV infection induces caspase 3-dependent apoptosis in Huh7.5 cells.** We first examined virus growth in Huh7.5 cells. HCV grew efficiently in the culture, and virus titers in the supernatant reached a plateau level at 2 days postinfection (Fig. 1A). Immunofluorescence analysis revealed that >95% of the cells were infected with HCV on the same day (Fig. 1B). To examine the possible impact of HCV infection on the cells, we measured the cell viability/proliferation at 0, 2, 4, and 6 days postinfection. As shown in Fig. 1C, the proliferation of HCV-infected cells was significantly slower than that of the mock-infected control. Similar results were obtained when the parental Huh7 cells were used for HCV infection (data not shown). The observed delay in cell proliferation was associated with an increase in cell death, seen as cell rounding and floating in the culture (data not shown) and in cellular DNA fragmentation (Fig. 1D). As DNA fragmentation is a hallmark of apoptosis, our data suggest that HCV infection induces apoptosis in Huh7.5 cells.

The J6/JFH1-P47 strain of HCV used in this study possesses adaptive mutations compared to the original strain (J6/JFH1-P1). Therefore, we compared the impacts of the two strains on cell viability/proliferation and DNA fragmentation. While both strains caused inhibition of cell proliferation and an increase in DNA fragmentation, J6/JFH1-P47 appeared to exert a stronger cytopathic effect than J6/JFH-P1 (data not shown).

To further verify that HCV infection induces apoptotic cell death, we analyzed caspase 3 activities in HCV-infected Huh7.5 cells and the mock-infected control. As shown in Fig. 2A, caspase 3 activities in HCV-infected cells increased to levels that were 2.2, 6.0, and 12 times higher than that in the control cells at 2, 4, and 6 days postinfection, respectively. We also examined HCV-induced caspase 3 activation by immunoblot analysis. Activation of caspase 3 requires proteolytic processing of its inactive proenzyme into the active 17-kDa and 12-kDa subunit proteins. The anti-caspase 3 antibody used in this analysis recognizes 35-kDa procaspase 3 and the 17-kDa subunit protein. At 6 days postinfection, activated caspase 3 was detected in HCV-infected cells but not in the mock-infected control (Fig. 2B, second row from the top). Analysis of the death substrate PARP, which is a key substrate for active caspase 3 (61), also demonstrated that the uncleaved PARP (116 kDa) was proteolytically cleaved to generate the 89-kDa fragment in HCV-infected cells but not in the mock-infected control (Fig. 2B, third row). Cleavage of PARP facilitates cellular disassembly and serves as a marker of cells undergoing apoptosis (44).

In order to further confirm these observations, indirect immunofluorescence staining was performed by using an anti-active caspase 3 antibody that specifically recognizes the newly exposed C terminus of the 17-kDa fragment of caspase 3 but not the inactive precursor form. As shown in Fig. 2C, the activated form of caspase 3 was clearly observed in HCV-infected cells but not in the mock-infected control at 6 days postinfection. The activation of caspase 3 was observed also at 4 days postinfection (data not shown). We found that caspase 3 activation was detectable in 12% and 21% of HCV antigen-positive cells at 4 and 6 days postinfection, respectively, whereas it was detectable only minimally in mock-infected cells at the same time points (Fig. 2D). These results strongly suggest that HCV-induced cell death is caused by caspase 3-dependent apoptosis. We also observed nuclear translocation of active caspase 3 in HCV-infected cells (Fig. 2E). This result is consistent with previous reports (28, 70) that activated caspase 3 is located not only in the cytoplasm but also in the nuclei of apoptotic cells. Concomitantly, nuclear condensation and shrinkage were clearly observed in the caspase 3-activated cells. As the activation and nuclear translocation of caspase 3 occur before the appearance of the nuclear change, not all caspase 3-activated cells exhibited the typical nuclear changes. Taken together, these results indicate that HCV-induced apoptosis is associated with activation and nuclear translocation of caspase 3.

**HCV infection induces the activation of the proapoptotic protein Bax.** The proteins of the Bcl-2 family are known to directly regulate mitochondrial membrane permeability and induction of apoptosis (63). Therefore, we examined the expression levels of proapoptotic proteins, such as Bax and Bak, and antiapoptotic protein Bcl-2 in HCV-infected Huh7.5 cells and the mock-infected control. The result showed that expression levels of Bak or Bcl-2 did not differ significantly between HCV-infected cells and the control. Interestingly, however, Bax accumulated on the mitochondria in HCV-infected cells to a larger extent than in the mock-infected control (Fig. 3A), with the average amount of mitochondrion-associated Bax in HCV-infected cells being 2.7 times larger than that in the control cells at 6 days postinfection (Fig. 3B).

In response to apoptotic stimuli, Bax undergoes a conformational change to expose its N and C termini, which facilitates translocation of the protein to the mitochondrial outer membrane (32). Thus, the conformational change of Bax represents a key step for its activation and subsequent apoptosis. We therefore investigated the possible conformational change of Bax in HCV-infected cells by using a conformation-specific NT antibody that specifically recognizes the Bax protein with an exposed N terminus. As shown in Fig. 3C, Bax staining with the conformation-specific NT antibody was readily detectable in HCV-infected cells at 6 days postinfection whereas there was no detectable staining with the same antibody in the mock-infected control. Moreover, the activated Bax was shown to be colocalized with MitoTracker, a marker for mitochondria, in HCV-infected cells. The conformational change of Bax was observed in 10% and 15% of HCV-infected cells at 4 and 6 days postinfection, respectively (Fig. 3D). This result was consistent with what was observed for caspase 3 activation in HCV-infected cells (Fig. 2D). Taken together, these results suggest that HCV infection triggers conformational change and mitochondrial accumulation of Bax, which lead to the activation of the mitochondrial apoptotic pathway.

**HCV infection induces the disruption of the mitochondrial transmembrane potential, release of cytochrome *c* from mitochondria, and activation of caspase 9.** The accumulation of Bax on the mitochondria is known to decrease the mitochondrial transmembrane potential and increase its permeability, which result in the release of cytochrome *c* and other key molecules from the mitochondria to the cytoplasm to activate caspase 9. Therefore, we examined the possible effect of HCV infection on mitochondrial transmembrane potential in Huh7.5 cells. Disruption of the mitochondrial transmembrane potential was indicated by decreased Rho123 retention and, hence, decreased fluorescence. As shown in Fig. 4, HCV-infected cells showed ~50% and ~70% reductions in Rho123 fluorescence intensity compared with the mock-infected control at 4 and 6 days postinfection, respectively.

Recent studies have indicated that loss of mitochondrial membrane potential leads to mitochondrial swelling, which is often associated with cell injury (27, 50). Also, we and other investigators have reported that HCV NS4A (43), core (53), and p7 (22) target mitochondria. We therefore analyzed the effect of HCV infection on mitochondrial morphology. Confocal fluorescence microscopic analysis using MitoTracker revealed that mitochondria began to undergo morphological changes at 4 days postinfection and that approximately 40% of HCV-infected cells exhibited mitochondrial swelling and/or aggregation compared with the mock-infected control at 6 days postinfection (Fig. 5A and B). It should also be noted that mitochondrial swelling and/or aggregation was seen in a region different from the "membranous web," where the HCV replication complexes accumulate to show stronger expression of

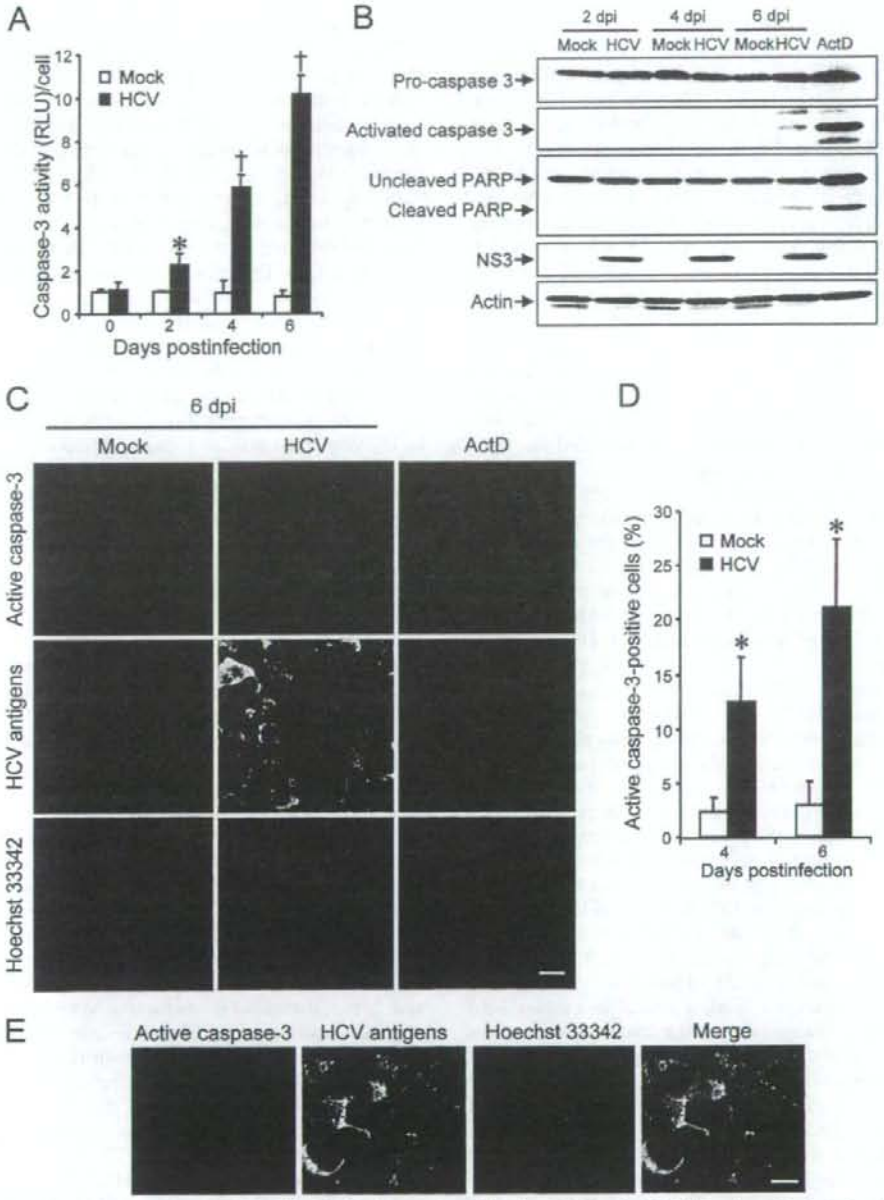


FIG. 2. HCV infection activates caspase 3 in Huh7.5 cells. (A) Caspase 3 activities in cells infected with HCV and mock-infected controls. The caspase 3 activity of the control cells at day 0 postinfection was arbitrarily expressed as 1.0. *, $P < 0.05$; †, $P < 0.01$ (compared with the control). Data represent means ± standard deviations (SD) of three independent experiments. (B) Immunoblot analysis to detect the activated form of caspase 3 (~17 kDa) and cleavage product of PARP (~85 kDa) in HCV-infected cells and the mock-infected control at 2, 4, and 6 days postinfection (dpi). Huh7.5 cells treated with actinomycin D (ActD; 50 ng/ml) for 30 h served as a positive control. Amounts of actin were measured as an internal control to verify an equal amount of sample loading. (C) Huh7.5 cells infected with HCV or mock infected were subjected to indirect immunofluorescence analysis at 6 dpi. Cells treated with ActD (50 ng/ml) for 30 h served as a positive control. After fixation and permeabilization, the cells were incubated with anti-active caspase 3 rabbit polyclonal antibody followed by Cy3-labeled donkey anti-rabbit IgG (top) and with an HCV-infected patient's serum followed by FITC-labeled goat anti-human IgG (middle). The cells were then stained with Hoechst 33342 for the nuclei (bottom). Scale bar, 20 μm. (D) Quantification of active caspase 3-expressing cells. The percentages of cells expressing active caspase 3 were determined for HCV-infected cultures and mock-infected controls. Data represent means ± SD of three independent experiments. *, $P < 0.05$, compared with the control. (E) Nuclear translocation of active caspase 3 in HCV-infected cells. Subcellular localization of active caspase 3 in HCV-infected cells was examined by indirect immunofluorescence analysis at 6 days postinfection as described in the legend for panel C. Scale bar, 5 μm.

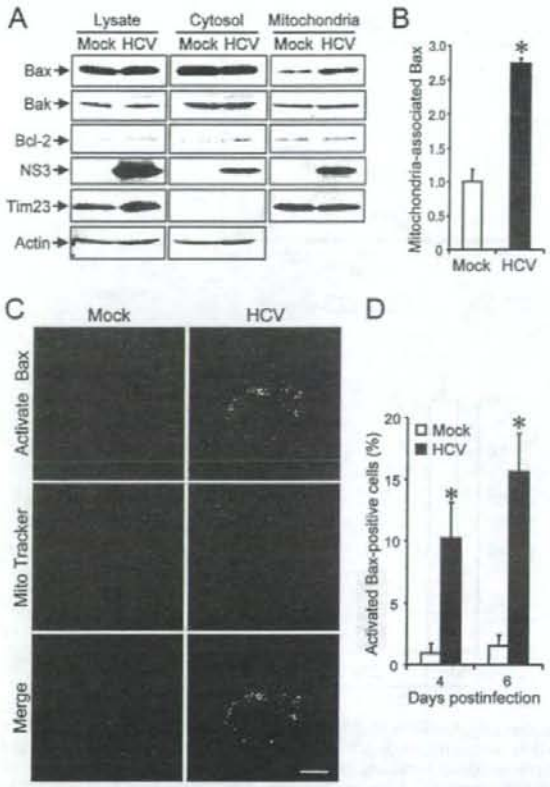


FIG. 3. HCV infection induces Bax activation in Huh7.5 cells. (A) Accumulation of Bax on the mitochondria in HCV-infected Huh7.5 cells. Cytosolic and mitochondrial fractions as well as whole-cell lysates were prepared from HCV-infected cells and the mock-infected control at 6 days postinfection and analyzed by immunoblotting using antibodies against Bax, Bak, Bcl-2, NS3, Tim23, and actin. Amounts of Tim23, a mitochondrion-specific protein, were measured to verify equal amounts of mitochondrial fractions. Amounts of actin were measured to verify equal amounts of whole-cell lysates and cytosolic fractions. (B) The intensities of the bands of mitochondrion-associated Bax in HCV-infected cells and the mock-infected control were quantified. The intensity of the mock-infected control was arbitrarily expressed as 1.0. Data represent means ± standard deviations (SD) of three independent experiments. *, $P < 0.01$, compared with the control. (C) Conformational change of Bax in HCV-infected cells. Huh7.5 cells infected with HCV and the mock-infected control were subjected to indirect immunofluorescence analysis at 6 days postinfection. After incubation with MitoTracker (middle row), the cells were incubated with an antibody specific for the N terminus of Bax (NT antibody), followed by Alexa Fluor 488-labeled goat anti-rabbit IgG (top row). Merged images are shown on the bottom. Scale bar, 10 μm. (D) Quantification of activated Bax-positive cells. The percentages of cells expressing activated Bax were determined for HCV-infected cultures and the mock-infected control. Data represent means ± SD of three independent experiments. *, $P < 0.01$, compared with the control.

HCV antigens. This observation implies the possibility that an indirect effect(s) of HCV infection, in addition to a direct effect of an HCV protein, as observed for NS3/4A (43), is involved in mitochondrial swelling and/or aggregation.

Electron microscopic analysis also demonstrated swelling and structural alterations of mitochondria in HCV-infected cells, whereas mitochondria remained intact in the mock-infected control (Fig. 5C). This result suggests a detrimental effect of HCV infection on the volume homeostasis and morphology of mitochondria and is consistent with previous observations that liver tissues from HCV-infected patients showed morphological changes in mitochondria (3).

Mitochondrial swelling and the morphological change of mitochondrial cristae are associated with cytochrome *c* release (27, 54). We then examined the effect of HCV infection on cytochrome *c* release in Huh7.5 cells. The result clearly demonstrated cytochrome *c* release from the mitochondria to the cytoplasm in HCV-infected cells but not in the mock-infected control (Fig. 6A). The release of cytochrome *c* from mitochondria is known to induce activation of caspase 9 (31). We then analyzed caspase 9 activities in the cells. As shown in Fig. 6B, caspase 9 activities in HCV-infected cells increased to levels that were ca. five times higher than that in the control cells at 4 and 6 days postinfection.

**HCV infection induces a marginal degree of caspase 8 activation.** In addition to the mitochondrial death (intrinsic) pathway described above, the extrinsic cell death pathway, which is initiated by the TNF family members and mediated by activated caspase 8 (31, 62), is also the focus of attention in the study of apoptosis. Therefore, we examined caspase 8 activities in HCV-infected cells and the mock-infected control. As shown in Fig. 6C, caspase 8 activities in HCV-infected cells increased to a level that was ca. two times higher than that in the control cells at 4 and 6 days postinfection. This increase was much smaller than that observed for caspase 9 activation (Fig. 6B).

**HCV infection induces increased production of mitochondrial reactive oxygen species (ROS).** The production of ROS, such as superoxide, by mitochondria is the major cause of cellular oxidative stress (8), and a possible link between ROS production and Bax activation has been reported (18, 42). Therefore, we next examined the mitochondrial ROS production in HCV- and mock-infected cells by using MitoSOX, a fluorescent probe specific for superoxide that selectively accumulates in the mitochondrial compartment. As shown in Fig. 7A and B, approximately 25% of HCV-infected cells displayed a much higher signal than did the mock-infected control. This result suggests that oxidative stress is induced by HCV infection.

**HCV infection does not induce ER stress.** It is well known that HCV nonstructural proteins form the replication complex on the endoplasmic reticulum (ER) membrane (4, 19, 39, 46). It was recently reported that HCV infection (55) as well as the transfection of the full-length HCV replicon (17) and the expression of the entire HCV polyprotein (14) induced an ER stress response. Therefore, we tested whether HCV infection in our system induces ER stress. We adopted increased expression of GRP78 and GRP94 as indicators of ER stress (34) and, as a positive control, used tunicamycin to induce ER stress (20, 25). As had been expected, the expression levels of GRP78 and GRP94 were markedly increased in Huh7.5 cells when cells were treated with tunicamycin for 48 h (Fig. 8, right). On the other hand, HCV infection did not alter expression levels of GRP78 or GRP94 at 2, 4, or 6 days postinfection compared

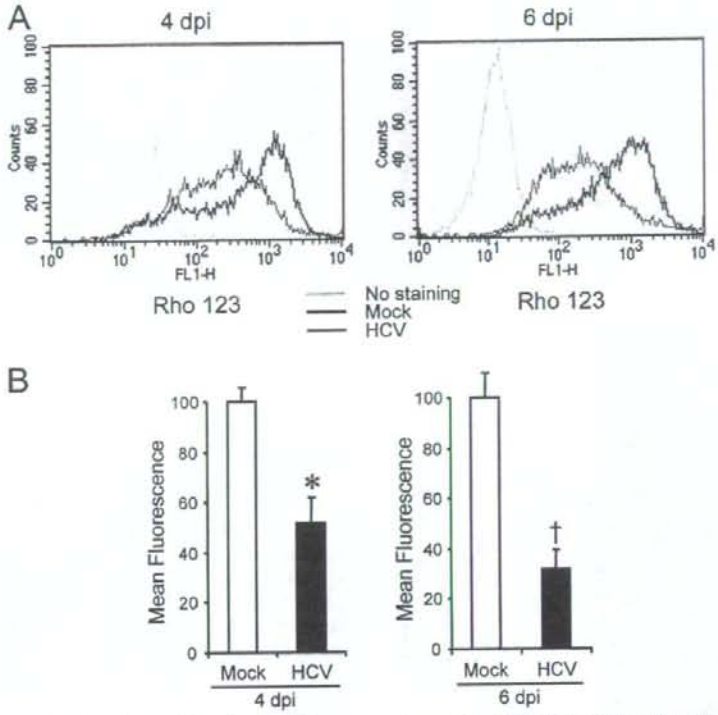


FIG. 4. HCV infection induces disruption of the mitochondrial transmembrane potential in Huh7.5 cells. (A) Huh7.5 cells infected with HCV and the mock-infected control were stained with Rho123 and subjected to flow cytometric analysis to measure the mitochondrial transmembrane potential at 4 and 6 days postinfection (dpi). The red and black lines represent Rho123 staining of HCV-infected cells and the mock-infected control, respectively. The green profiles represent staining of the cells with PBS alone. (B) Mean fluorescence intensities of HCV-infected cells and the mock-infected control at 4 and 6 dpi. Data represent means ± standard deviations (SD) of three independent experiments. *, $P < 0.05$; †, $P < 0.01$ (compared with the control).

with those for the mock-infected control (Fig. 8). This result suggests that ER stress, if there is any, is marginal and does not play an important role in HCV-induced apoptosis in Huh7.5 cells.

## DISCUSSION

The mitochondrion is an important organelle for cell survival and death and plays a crucial role in regulating apoptosis. An increasing body of evidence suggests that apoptosis occurs in the livers of HCV-infected patients (1, 2, 9) and that HCV-associated apoptosis involves, at least partly, a mitochondrion-mediated pathway (2). In those clinical settings, however, it is not clear whether apoptosis is mediated by host immune responses through the activity of cytotoxic T lymphocytes or whether it is mediated directly by HCV replication and/or protein expression itself. In experimental settings, ectopic expression of HCV core (13, 36), E2 (12), and NS4A (43) has been shown to induce mitochondrion-mediated apoptosis in cultured cells. However, these observations need to be verified in the context of virus replication. The recent development of an efficient HCV infection system in cell culture (37, 66, 71) has allowed us to investigate whether HCV replication directly causes apoptosis. In the present study, we have demonstrated that HCV infection induces Bax-triggered, mitochondrion-mediated, caspase 3-dependent apoptosis, as evidenced by increased accumulation of Bax on mitochondria and its conformational change (Fig. 3), decreased mitochondrial transmembrane potential (Fig. 4), and mitochondrial swelling (Fig. 5), which lead to the release of cytochrome c from the mitochondria (Fig. 6A) and subsequent activation of caspase 9 and caspase 3 (Fig. 6B and 2, respectively).

We also observed increased production of mitochondrial superoxide in HCV-infected cells (Fig. 7). This result is consistent with previous observations that expression of the entire HCV polyprotein (47) or HCV replication (60) enhanced production of ROS, including superoxide, through deregulation of mitochondrial calcium homeostasis. ROS, which are produced through the mitochondrial respiratory chain (8), were reported to trigger conformational change, dimerization, and mitochondrial translocation of Bax (18, 42). It is likely, therefore, that activation of Bax in HCV-infected cells is mediated, at least partly, through increased production of ROS in the mitochondria. Kim et al. (29) reported that ROS is a potent activator of c-Jun N-terminal protein kinase, which can phosphorylate Bax, leading to its activation and mitochondrial translocation. In

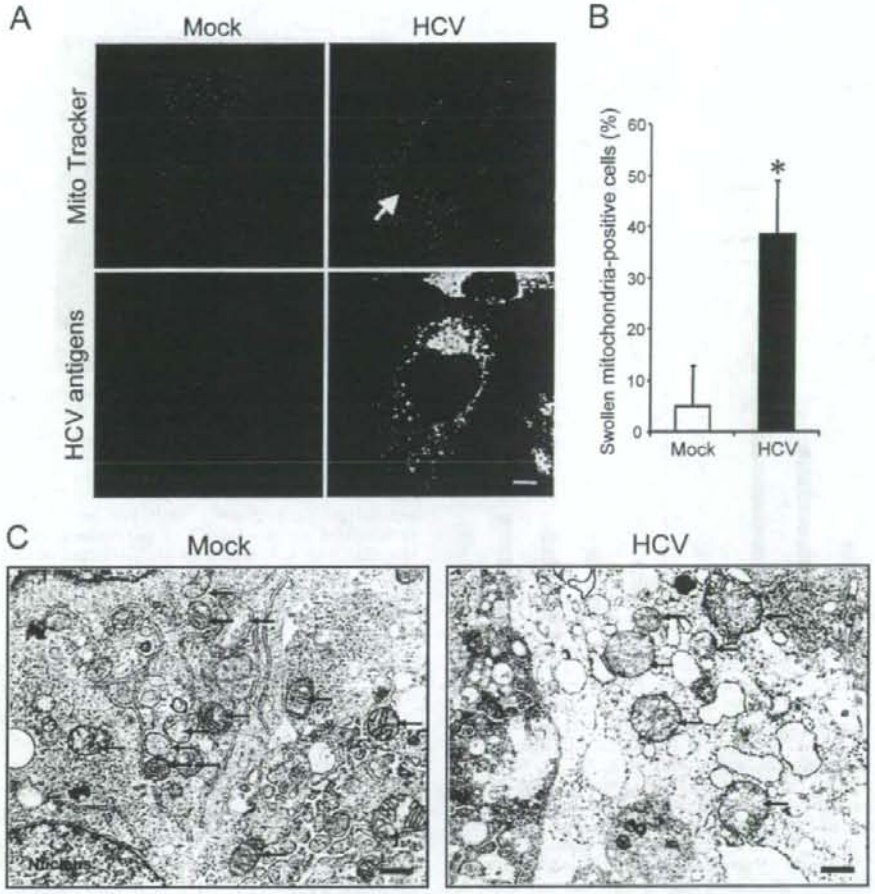


FIG. 5. HCV infection induces mitochondrial morphology changes in Huh7.5 cells. (A) Fluorescence microscopy analysis. Mitochondrial morphologies of HCV-infected cells and the mock-infected control at 6 days postinfection were examined by confocal microscopy. The cells were directly incubated with MitoTracker (upper row) and then stained for HCV antigens by using an HCV-infected patient's serum, followed by FITC-labeled goat anti-human IgG (bottom row). Scale bar, 5 μm. (B) Quantification of swollen mitochondrion-positive cells. The percentages of cells exhibiting swollen and/or aggregated mitochondria were determined for HCV-infected cultures and the mock-infected control. Data represent means ± standard deviations of three independent experiments. *, $P < 0.01$, compared with the control. (C) Electron microscopic analysis. Mitochondrial morphologies of HCV-infected cells and the mock-infected control at 6 days postinfection were examined by electron microscopy. Arrows indicate mitochondria. Scale bar, 1 μm.

this connection, HCV core protein has been shown to play a role in generating mitochondrial ROS (30). It was also reported that HCV core protein bound to the 14-3-3ε protein to dissociate Bax from the Bax/14-3-3ε complex, thereby promoting the Bax translocation to the mitochondria (36).

In addition to the caspase 9 activation that is mediated through the mitochondrial death (intrinsic) pathway, caspase 8 activation was seen in HCV-infected cells, though to a lesser extent (Fig. 6B and C). Caspase 8 is a key component of the extrinsic death pathway initiated by the TNF family members (31, 62). This pathway involves death receptors, such as Fas, TNF receptor, and TNF-related apoptosis-inducing ligand (TRAIL) receptors, which transduce signals to induce apoptosis upon binding to their respective ligands (52). In HCV-infected patients, the Fas-mediated signal pathway is involved in apoptosis of virus-infected hepatocytes (24). It was also reported that HCV (JFH1 strain) infection induced apoptosis through a TRAIL-mediated pathway in LH86 cells (72). On the other hand, a caspase 9-mediated activation of caspase 8, which is considered a cross talk between the intrinsic and the extrinsic death pathways, in certain cell systems was also reported (10, 11, 65). Whether the observed caspase 8 activation in HCV-infected cells was mediated through the extrinsic death pathway initiated by a cytokine(s) produced in the culture or whether it was mediated through the cross talk between the intrinsic and the extrinsic death pathways awaits further investigation. In this connection, activated caspase 8 is known to cleave the proapoptotic protein Bid to generate the Bid

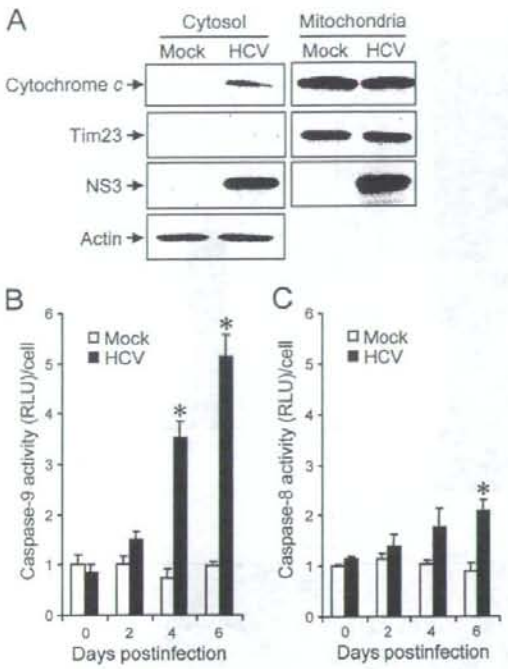


FIG. 6. HCV infection induces cytochrome *c* release and caspase 9 activation in Huh7.5 cells. (A) Cytochrome *c* release. Mitochondrial and cytosolic fractions were prepared from HCV-infected cells and the mock-infected control at 6 days postinfection and analyzed by immunoblotting using antibodies against cytochrome *c*, Tim23, NS3, and actin. Can Get Signal (Toyobo, Osaka, Japan) was used to obtain stronger signals for cytochrome *c*. Amounts of Tim23 and actin were measured to verify equal amounts of mitochondrial and cytosolic fractions, respectively. Also, Tim23 was used to show successful separation of mitochondria. (B) Caspase 9 activation. Caspase 9 activities in cells infected with HCV and mock-infected controls were measured at 0, 2, 4, and 6 days postinfection. The caspase 9 activity of the control cells at day 0 postinfection was arbitrarily expressed as 1.0. Data represent means ± standard deviations (SD) of three independent experiments. *, $P < 0.05$, compared with the control. (C) HCV infection induces a marginal degree of caspase 8 activation. Caspase 8 activities in cells infected with HCV and mock-infected controls were measured at 0, 2, 4, and 6 days postinfection. The caspase 8 activity of the control cells at day 0 postinfection was arbitrarily expressed as 1.0. Data represent means ± SD of three independent experiments. *, $P < 0.05$, compared with the control.

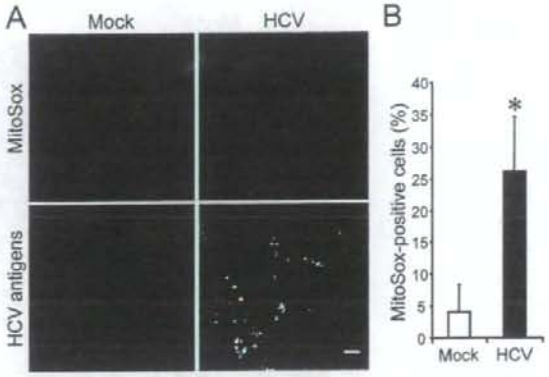


FIG. 7. HCV infection induces increased production of mitochondrial superoxide in Huh7.5 cells. (A) Mitochondrial superoxide production in HCV-infected cells and the mock-infected control was examined at 6 days postinfection. Cells were directly incubated with MitoSOX (upper row) and then stained for HCV antigens by using an HCV-infected patient's serum, followed by FITC-labeled goat anti-human IgG (bottom row). Scale bar, 10 μm. (B) Quantification of MitoSOX-stained cells. The percentages of cells stained with MitoSOX were determined for HCV-infected cultures and the mock-infected control. Data represent means ± standard deviations of three independent experiments. *, $P < 0.05$, compared with the control.

cleavage product truncated Bid (tBid), which facilitates the activation of Bax (63, 68). Under our experimental conditions, however, tBid was barely detected in HCV-infected cells even at 6 days postinfection (data not shown). It is thus likely that caspase 8 activation is marginal and is not the primary cause of Bax activation in our experimental system.

HCV protein expression and HCV RNA replication take place primarily in the ER or an ER-like membranous structure (39, 46). Like other members of the family *Flaviviridae*, such as dengue virus (69), Japanese encephalitis virus (69), West Nile virus (41), and bovine viral diarrhea virus (26), HCV has been reported to induce ER stress in the host cells (5, 14, 17, 55, 60). ER stress is triggered by perturbations in normal ER function, such as the accumulation of unfolded or misfolded proteins in the lumen. On the other hand, in response to ER stress, the unfolded protein response (UPR) is activated to alleviate the ER stress by stimulating protein folding and degradation in the ER as well as by inhibiting protein synthesis (7). The UPR of the host cell is disadvantageous for progeny virus production and may therefore be considered an antiviral host cell response. It was reported that, to counteract the disadvantageous UPR so as to maintain viral protein synthesis, HCV RNA replication suppressed the IRE1-XBP1 pathway, which is responsible for protein degradation upon UPR (59). Also, HCV E2 was shown to inhibit the double-stranded RNA-activated protein kinase-like ER-resident kinase (PERK), which attenuates protein synthesis during ER stress by phosphorylating the alpha subunit of eukaryotic translation initiation factor 2 (45). It is reasonable, therefore, to assume that HCV-infected cells may not necessarily exhibit typical responses to ER stress. In fact, our results revealed that HCV infection in Huh7.5 cells did not enhance

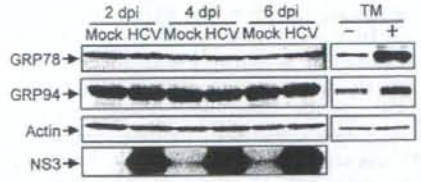


FIG. 8. HCV infection does not induce ER stress in Huh7.5 cells. Huh7.5 cells infected with HCV and mock-infected controls were harvested at 2, 4, and 6 days postinfection (dpi), and the whole-cell lysates were subjected to immunoblot analysis using antibodies against GRP78, GRP94, NS3, and actin. Amounts of actin were measured to verify equal amounts of sample loading. Huh7.5 cells treated with tunicamycin (TM; 5 μg/ml) for 48 h served as a positive control.

expression of GRP78 and GRP94, which are ER stress-induced chaperone proteins (Fig. 8). Our result thus implies the possibility that ER stress is not crucially involved in HCV-induced apoptosis in Huh7.5 cells. Taking advantage of this phenomenon, we could demonstrate that an ER stress-independent, mitochondrion-mediated pathway plays an important role in HCV-induced apoptosis. In this connection, Korenaga et al. (30) reported that HCV core protein increased ROS production in isolated mitochondria, independently of ER stress, by selectively inhibiting electron transport complex I activity.

In this study, we observed that increased ROS production, Bax activation, and caspase 3 activation were detectable in approximately 15% to 25% of HCV antigen-positive Huh7.5cells at 6 days postinfection (Fig. 7B, 3D, and 2D, respectively). On the other hand, >90% of the cells in the cultures were confirmed positive for HCV antigens (Fig. 1B). These results imply the possibility that HCV establishes persistent infection in Huh7.5 cells, with a minor fraction of virus-infected cells beginning to undergo apoptosis after a prolonged period of time. Alternatively, it is possible that Huh7.5 cells, though being derived from a cell line (6), are a mixture of two sublineages, with one sublineage being apoptosis prone and the other apoptosis resistant. To test the latter possibility, further cloning of Huh7.5 cells is now under way in our laboratory.

In conclusion, our present results collectively suggest that HCV infection induces apoptosis through a Bax-triggered, mitochondrion-mediated, caspase 3-dependent pathway.

## ACKNOWLEDGMENTS

We are grateful to C. M. Rice (Center for the Study of Hepatitis C, The Rockefeller University) for providing pFL-J6/JFH1 and Huh7.5 cells.

This work was supported in part by grants-in-aid for scientific research from the Ministry of Education, Culture, Sports, Science and Technology (MEXT) and the Ministry of Health, Labor and Welfare, Japan.

This study was carried out as part of the Program of Founding Research Centers for Emerging and Reemerging Infectious Diseases, MEXT, Japan. This study was also part of the 21st Century Center of Excellence Program at Kobe University Graduate School of Medicine.

## REFERENCES

1. **Bantel, H., A. Lügering, C. Poremba, N. Lügering, J. Held, W. Domschke, and K. Schulze-Osthoff.** 2001. Caspase activation correlates with the degree of inflammatory liver injury in chronic hepatitis C virus infection. Hepatology **34**:758–767.
2. **Bantel, H., and K. Schulze-Osthoff.** 2003. Apoptosis in hepatitis C virus infection. Cell Death Differ. **10**:S48–S58.
3. **Barbaro, G., G. Di Lorenzo, A. Asti, M. Ribersani, G. Belloni, B. Grisorio, G. Filice, and G. Barbarini.** 1999. Hepatocellular mitochondrial alterations in patients with chronic hepatitis C: ultrastructural and biochemical findings. Am. J. Gastroenterol. **94**:2198–2205.
4. **Bartenschlager, R., M. Frese, and T. Pietschmann.** 2004. Novel insights into hepatitis C virus replication and persistence. Adv. Virus Res. **63**:171–180.
5. **Benali-Furet, N. L., M. Chami, L. Houel, F. De Giorgi, F. Vernejoul, D. Lagorce, L. Buscail, R. Bartenschlager, F. Ichas, R. Rizzuto, and P. Paterlini-Bréchot.** 2005. Hepatitis C virus core triggers apoptosis in liver cells by inducing ER stress and ER calcium depletion. Oncogene **24**:4921–4933.
6. **Blight, K. J., J. A. McKeating, and C. M. Rice.** 2002. Highly permissive cell lines for subgenomic and genomic hepatitis C virus RNA replication. J. Virol. **76**:13001–13014.
7. **Boyce, M., and J. Yuan.** 2006. Cellular response to endoplasmic reticulum stress: a matter of life or death. Cell Death Differ. **13**:363–373.
8. **Brookes, P. S.** 2005. Mitochondrial $H^+$ leak and ROS generation: an odd couple. Free Radic. Biol. Med. **38**:12–23.
9. **Calabrese, F., P. Pontisso, E. Pettenazzo, L. Benvegnù, A. Vario, L. Chemello, A. Alberti, and M. Valente.** 2000. Liver cell apoptosis in chronic hepatitis C correlates with histological but not biochemical activity or serum HCV-RNA levels. Hepatology **31**:1153–1159.
10. **Camacho-Leal, P., and C. P. Stanners.** 2008. The human carcinoembryonic antigen (CEA) GPI anchor mediates anoikis inhibition by inactivation of the intrinsic death pathway. Oncogene **27**:1545–1553.
11. **Chae, Y. J., H. S. Kim, H. Rhim, B. E. Kim, S. W. Jeong, and I. K. Kim.** 2001. Activation of caspase-8 in 3-deazaadenosine-induced apoptosis of U-937 cells occurs downstream of caspase-3 and caspase-9 without Fas receptor-ligand interaction. Exp. Mol. Med. **4**:284–292.
12. **Chiou, H. L., Y. S. Hsieh, M. R. Hsieh, and T. Y. Chen.** 2006. HCV E2 may induce apoptosis of Huh-7 cells via a mitochondrial-related caspase pathway. Biochem. Biophys. Res. Commun. **345**:453–458.
13. **Chou, A. H., H. F. Tsai, Y. Y. Wu, C. Y. Hu, L. H. Hwang, P. I. Hsu, and P. N. Hsu.** 2005. Hepatitis C virus core protein modulates TRAIL-mediated apoptosis by enhancing Bid cleavage and activation of mitochondria apoptosis signaling pathway. J. Immunol. **174**:2160–2166.
14. **Christen, V., S. Treves, F. H. Duong, and M. H. Heim.** 2007. Activation of endoplasmic reticulum stress response by hepatitis viruses up-regulates protein phosphatase 2A. Hepatology **46**:558–565.
15. **Ciccaglione, A. R., C. Marcantonio, A. Costantino, M. Equestre, and M. Rapicetta.** 2003. Expression of HCV E1 protein in baculovirus-infected cells: effects on cell viability and apoptosis induction. Intervirology **46**:121–126.
16. **Ciccaglione, A. R., C. Marcantonio, E. Tritarelli, M. Equestre, F. Magurano, A. Costantino, L. Nicoletti, and M. Rapicetta.** 2004. The transmembrane domain of hepatitis C virus E1 glycoprotein induces cell death. Virus Res. **104**:1–9.
17. **Ciccaglione, A. R., C. Marcantonio, E. Tritarelli, M. Equestre, F. Venditteli, A. Costantino, A. Geraci, and M. Rapicetta.** 2007. Activation of the ER stress gene gadd153 by hepatitis C virus sensitizes cells to oxidant injury. Virus Res. **126**:128–138.
18. **D'Alessio, M., M. De Nicola, S. Coppola, G. Gualandi, L. Pugliese, C. Cerella, S. Cristofanon, P. Civitareale, M. R. Ciriolo, A. Bergamaschi, A. Magrini, and L. Ghibelli.** 2005. Oxidative Bax dimerization promotes its translocation to mitochondria independently of apoptosis. FASEB J. **19**: 1504–1506.
19. **Egger, D., B. Wölk, R. Gosert, L. Bianchi, H. E. Blum, D. Moradpour, and K. Bienz.** 2002. Expression of hepatitis C virus proteins induces distinct membrane alterations including a candidate viral replication complex. J. Virol. **76**:5974–5984.
20. **Elbein, A. D.** 1987. Inhibitors of the biosynthesis and processing of N-linked oligosaccharide chains. Annu. Rev. Biochem. **56**:497–534.
21. **Erdtmann, L., N. Franck, H. Lerat, J. Le Seyec, D. Gilot, I. Cannie, P. Gripon, U. Hibner, and C. Guguen-Guillouzo.** 2003. The hepatitis C virus NS2 protein is an inhibitor of CIDE-B-induced apoptosis. J. Biol. Chem. **278**:18256–18264.
22. **Griffin, S., D. Clarke, C. McCormick, D. Rowlands, and M. Harris.** 2005. Signal peptide cleavage and internal targeting signals direct the hepatitis C virus p7 protein to distinct intracellular membranes. J. Virol. **79**:15525–15536.
23. **Hidajat, R., M. Nagano-Fujii, L. Deng, M. Tanaka, Y. Takigawa, S. Kitazawa, and H. Hotta.** 2005. Hepatitis C virus NS3 protein interacts with ELKS-β and ELKS-α, members of a novel protein family involved in intracellular transport and secretory pathways. J. Gen. Virol. **86**:2197–2208.
24. **Jarmay, K., G. Karacsony, Z. Ozsvar, I. Nagy, J. Lonovics, and Z. Schaff.** 2002. Assessment of histological feature in chronic hepatitis C. Hepatogastroenterology **49**:239–243.
25. **Jiang, C. C., L. H. Chen, S. Gillespie, K. A. Kiejda, N. Mhaidat, Y. F. Wang, R. Thorne, X. D. Zhang, and P. Hersey.** 2007. Tunicamycin sensitizes human melanoma cells to tumor necrosis factor-related apoptosis-inducing ligand-induced apoptosis by up-regulation of TRAIL-R2 via the unfolded protein response. Cancer Res. **67**:5880–5888.
26. **Jordan, R., L. Wang, T. M. Graczyk, T. M. Block, and P. R. Romano.** 2002. Replication of a cytopathic strain of bovine viral diarrhea virus activates PERK and induces endoplasmic reticulum stress-mediated apoptosis of MDBK cells. J. Virol. **76**:9588–9599.
27. **Kaasik, A., D. Safiulina, A. Zharkovsky, and V. Veksler.** 2007. Regulation of mitochondrial matrix volume. Am. J. Physiol. Cell Physiol. **292**:C157–C163.
28. **Kamada, S., U. Kikkawa, Y. Tsujimoto, and T. Hunter.** 2005. Nuclear translocation of caspase-3 is dependent on its proteolytic activation and recognition of a substrate-like protein(s). J. Biol. Chem. **280**:857–860.
29. **Kim, B. J., S. W. Ryu, and B. J. Song.** 2006. JNK- and p38 kinase-mediated phosphorylation of Bax leads to its activation and mitochondrial translocation and to apoptosis of human hepatoma HepG2 cells. J. Biol. Chem. **281**:21256–21265.
30. **Korenaga, M., T. Wang, Y. Li, L. A. Showalter, T. Chan, J. Sun, and S. A. Weinman.** 2005. Hepatitis C virus core protein inhibits mitochondrial electron transport and increases reactive oxygen species (ROS) production. J. Biol. Chem. **280**:37481–37488.
31. **Kumar, S.** 2007. Caspase function in programmed cell death. Cell Death Differ. **14**:32–43.
32. **Lalier, L., P. F. Cartron, P. Juin, S. Nedelkina, S. Manon, B. Bechinger, and**

F. M. Vallette. 2007. Bax activation and mitochondrial insertion during apoptosis. Apoptosis 12:887–896.
33. Lan, K. H., M. L. Sheu, S. J. Hwang, S. H. Yen, S. Y. Chen, J. C. Wu, Y. J. Wang, N. Kato, M. Omata, F. Y. Chang, and S. D. Lee. 2002. HCV NS5A interacts with p53 and inhibits p53-mediated apoptosis. Oncogene 21:4801–4811.
34. Lee, A. S. 2001. The glucose-regulated proteins: stress induction and clinical applications. Trends Biochem. Sci. 26:504–510.
35. Lee, S. H., Y. K. Kim, C. S. Kim, S. K. Seol, J. Kim, S. Cho, Y. L. Song, R. Bartenschlager, and S. K. Jang. 2005. E2 of hepatitis C virus inhibits apoptosis. J. Immunol. 175:8226–8235.
36. Lee, S. K., S. O. Park, C. O. Joe, and Y. S. Kim. 2007. Interaction of HCV core protein with 14-3-3ε protein releases Bax to activate apoptosis. Biochem. Biophys. Res. Commun. 352:756–762.
37. Lindenbach, B. D., M. J. Evans, A. J. Syder, B. Wölk, T. L. Tellinghuisen, C. C. Liu, T. Maruyama, R. O. Hynes, D. R. Burton, J. A. McKeating, and C. M. Rice. 2005. Complete replication of hepatitis C virus in cell culture. Science 309:623–626.
38. Lindenbach, B. D., P. Meuleman, A. Ploss, T. Vanwolleghem, A. J. Syder, J. A. McKeating, R. E. Lanford, S. M. Feinstone, M. E. Major, G. Leroux-Roels, and C. M. Rice. 2006. Cell culture-grown hepatitis C virus is infectious in vivo and can be recultured in vitro. Proc. Natl. Acad. Sci. USA 103:3805–3809.
39. Lindenbach, B. D., and C. M. Rice. 2005. Unravelling hepatitis C virus replication from genome to function. Nature 436:933–938.
40. Marusawa, H., M. Hijikata, T. Chiba, and K. Shimotohno. 1999. Hepatitis C virus core protein inhibits Fas- and tumor necrosis factor alpha-mediated apoptosis via NF-κB activation. J. Virol. 73:4713–4720.
41. Medigeshi, G. R., A. M. Lancaster, A. J. Hirsch, T. Briese, W. I. Lipkin, V. Defilippis, K. Früh, P. W. Mason, J. Nikolich-Zugich, and J. A. Nelson. 2007. West Nile virus infection activates the unfolded protein response, leading to CHOP induction and apoptosis. J. Virol. 81:10849–10860.
42. Nie, C., C. Tian, L. Zhao, P. X. Petit, M. Mehrpour, and Q. Chen. 2008. Cysteine 62 of Bax is critical for its conformational activation and its pro-apoptotic activity in response to $H_2O_2$-induced apoptosis. J. Biol. Chem. 283:15359–15369.
43. Nomura-Takigawa, Y., M. Nagano-Fujii, L. Deng, S. Kitazawa, S. Ishido, K. Sada, and H. Hotta. 2006. Non-structural protein 4A of Hepatitis C virus accumulates on mitochondria and renders the cells prone to undergoing mitochondria-mediated apoptosis. J. Gen. Virol. 87:1935–1945.
44. Oliver, F. J., G. de la Rubia, V. Rolli, M. C. Ruiz-Ruiz, G. de Murcia, and J. M. Murcia. 1998. Importance of poly(ADP-ribose) polymerase and its cleavage in apoptosis. J. Biol. Chem. 273:33533–33539.
45. Pavio, N., P. R. Romano, T. M. Graczyk, S. M. Feinstone, and D. R. Taylor. 2003. Protein synthesis and endoplasmic reticulum stress can be modulated by the hepatitis C virus envelope protein E2 through the eukaryotic initiation factor 2α kinase PERK. J. Virol. 77:3578–3585.
46. Pawlotsky, J. M., S. Chevaliez, and J. G. McHutchison. 2007. The hepatitis C virus life cycle as a target for new antiviral therapies. Gastroenterology. 132:1979–1998.
47. Piccoli, C., R. Scrima, G. Quarato, A. D'Aprile, M. Ripoli, L. Lecce, D. Boffoli, D. Moradpour, and N. Capitanio. 2007. Hepatitis C virus protein expression causes calcium-mediated mitochondrial bioenergetic dysfunction and nitro-oxidative stress. Hepatology 46:58–65.
48. Prikhod'ko, E. A., G. G. Prikhod'ko, R. M. Siegel, P. Thompson, M. E. Major, and J. I. Cohen. 2004. The NS3 protein of hepatitis C virus induces caspase-8-mediated apoptosis independent of its protease or helicase activities. Virology 329:53–67.
49. Ray, R. B., K. Meyer, R. Steele, A. Shrivastava, B. B. Aggarwal, and R. Ray. 1998. Inhibition of tumor necrosis factor (TNF-α)-mediated apoptosis by hepatitis C virus core protein. J. Biol. Chem. 273:2256–2259.
50. Safiulina, D., V. Veksler, A. Zharkovsky, and A. Kaasik. 2006. Loss of mitochondrial membrane potential is associated with increase in mitochondrial volume: physiological role in neurones. J. Cell. Physiol. 206:347–353.
51. Saito, K., K. Meyer, R. Warner, A. Basu, R. B. Ray, and R. Ray. 2006. Hepatitis C virus core protein inhibits tumor necrosis factor alpha-mediated apoptosis by a protective effect involving cellular FLICE inhibitory protein. J. Virol. 80:4372–4379.
52. Schulze-Osthoff, K., D. Ferrari, M. Los, S. Wesselborg, and M. E. Peter. 1998. Apoptosis signaling by death receptors. Eur. J. Biochem. 254:439–459.
53. Schwer, B., S. Ren, T. Pietschmann, J. Kartenbeck, K. Kaehlcke, R. Bartenschlager, T. S. Yen, and M. Ott. 2004. Targeting of hepatitis C virus core protein to mitochondria through a novel C-terminal localization motif. J. Virol. 78:7958–7968.
54. Scorrano, L., M. Ashiya, K. Buttle, S. Weiler, S. A. Oakes, C. A. Mannella, and S. J. Korsmeyer. 2002. A distinct pathway remodels mitochondrial cristae and mobilizes cytochrome c during apoptosis. Dev. Cell 2:55–67.
55. Sekine-Osajima, Y., N. Sakamoto, K. Mishima, M. Nakagawa, Y. Itsui, M. Tasaka, Y. Nishimura-Sakurai, C. H. Chen, T. Kanai, K. Tsuchiya, T. Wakita, N. Enomoto, and M. Watanabe. 2008. Development of plaque assays for hepatitis C virus-JFH1 strain and isolation of mutants with enhanced cytopathogenicity and replication capacity. Virology 371:71–85.
56. Shepard, C. W., L. Finelli, and M. J. Alter. 2005. Global epidemiology of hepatitis C virus infection. Lancet Infect. Dis. 5:558–567.
57. Siavoshian, S., J. D. Abraham, C. Thumann, M. P. Kieny, and C. Schuster. 2005. Hepatitis C virus core, NS3, NS5A, NS5B proteins induce apoptosis in mature dendritic cells. J. Med. Virol. 75:402–411.
58. Tanaka, M., M. Nagano-Fujii, L. Deng, S. Ishido, K. Sada, and H. Hotta. 2006. Single-point mutations of hepatitis C virus that impair p53 interaction and anti-apoptotic activity of NS3. Biochem. Biophys. Res. Commun. 340:792–799.
59. Tardif, K. D., K. Mori, R. J. Kaufman, and A. Siddiqui. 2004. Hepatitis C virus suppresses the IRE1-XBP1 pathway of the unfolded protein response. J. Biol. Chem. 279:17158–17164.
60. Tardif, K. D., G. Waris, and A. Siddiqui. 2005. Hepatitis C virus, ER stress, and oxidative stress. Trends Microbiol. 13:159–163.
61. Tewari, M., L. T. Quan, K. O'Rourke, S. Desnoyers, Z. Zeng, D. R. Beidler, G. G. Poirier, G. S. Salvesen, and V. M. Dixit. 1995. Yama/CPP32 beta, a mammalian homolog of CED-3, is a CrmA-inhibitable protease that cleaves the death substrate poly (ADP-ribose) polymerase. Cell 81:801–809.
62. Thorburn, A. 2004. Death receptor-induced cell killing. Cell. Signal. 16:139–144.
63. Tsujimoto, Y. 2003. Cell death regulation by the Bcl-2 protein family in the mitochondria. J. Cell. Physiol. 195:158–167.
64. Upton, J. P., A. J. Valentijn, L. Zhang, and A. P. Gilmore. 2007. The N-terminal conformation of Bax regulates cell commitment to apoptosis. Cell Death Differ. 14:932–942.
65. Viswanath, V., Y. Wu, R. Boonplueang, S. Chen, F. F. Stevenson, F. Yantiri, L. Yang, M. F. Beal, and J. K. Andersen. 2001. Caspase-9 activation results in downstream caspase-8 activation and bid cleavage in 1-methyl-4-phenyl-1,2,3,6-tetrahydropyridine-induced Parkinson's disease. J. Neurosci. 21:9519–9528.
66. Wakita, T., T. Pietschmann, T. Kato, T. Date, M. Miyamoto, Z. Zhao, K. Murthy, A. Habermann, H. G. Kräusslich, M. Mizokami, R. Bartenschlager, and T. J. Liang. 2005. Production of infectious hepatitis C virus in tissue culture from a cloned viral genome. Nat. Med. 11:791–796.
67. Wang, J., W. Tong, X. Zhang, L. Chen, Z. Yi, T. Pan, Y. Hu, L. Xiang, and Z. Yuan. 2006. Hepatitis C virus non-structural protein NS5A interacts with FKBP38 and inhibits apoptosis in Huh7 hepatoma cells. FEBS Lett. 580:4392–4400.
68. Wei, M. C., W. X. Zong, E. H. Cheng, T. Lindsten, V. Panoutsakopoulou, A. J. Ross, K. A. Roth, G. R. MacGregor, C. B. Thompson, and S. J. Korsmeyer. 2001. Proapoptotic BAX and BAK: a requisite gateway to mitochondrial dysfunction and death. Science 292:727–730.
69. Yu, C. Y., Y. W. Hsu, C. L. Liao, and Y. L. Lin. 2006. Flavivirus infection activates the XBP1 pathway of the unfolded protein response to cope with endoplasmic reticulum stress. J. Virol. 80:11868–11880.
70. Zhivotovsky, B., A. Samali, A. Gahm, and S. Orrenius. 1999. Caspases: their intracellular localization and translocation during apoptosis. Cell Death Differ. 6:644–651.
71. Zhong, J., P. Gastaminza, G. Cheng, S. Kapadia, T. Kato, D. R. Burton, S. F. Wieland, S. L. Uprichard, T. Wakita, and F. V. Chisari. 2005. Robust hepatitis C virus infection in vitro. Proc. Natl. Acad. Sci. USA 102:9294–9299.
72. Zhu, H., H. Dong, E. Eksioglu, A. Hemming, M. Cao, J. M. Crawford, D. R. Nelson, and C. Liu. 2007. Hepatitis C virus triggers apoptosis of a newly developed hepatoma cell line through antiviral defense system. Gastroenterology 133:1649–1659.
73. Zhu, N., A. Khoshnan, R. Schneider, M. Matsumoto, G. Dennert, C. Ware, and M. M. C. Lai. 1998. Hepatitis C virus core protein binds to the cytoplasmic domain of tumor necrosis factor (TNF) receptor 1 and enhances TNF-induced apoptosis. J. Virol. 72:3691–3697.

＜原　著＞

# 1b型高ウイルス量高齢者C型慢性肝炎に対するPEG IFNα-2b/リバビリン治療（併用療法）の検討

金　守良[1)*]　井本　勉[1)]　婦木　秀一[1)]　金　啓二[2)]
谷口　美幸[3)]　長野　基子[4)]　堀田　博[4)]　勝二　郁夫[4)]
寒原　芳浩[5)]　前川　陽子[6)]　工藤　正俊[7)]　林　祥剛[8)]

要旨：1b型高ウイルスC型慢性肝炎の65歳以上（高齢群）23名（平均年齢69.4歳）と65歳未満（非高齢群）52名（平均年齢53.5歳）を対象にIFNα2b/リバビリン併用療法を比較検討した．著効率と中断率は高齢群37.5%（6/16），30.4%（7/23），非高齢群50%（20/40），23.1%（12/52）で有意差はなく，HCVコア抗原減少率，2-5AS応答率も両群間に有意差を認めなかった．高齢群では著効例は非著効例に比して開始時のAFP値が有意に低値であった（P<0.01），高齢群では著効・非著効を問わず治療前後でAFP値は有意に低下しており（開始時10.1±9.55 ng/ml，終了時5.18±4.52 ng/ml（P<0.05）），治療により発癌抑制がもたらされた可能性が考えられた．よって，高齢群においては，たとえ著効に至らない場合であっても治療の完遂が重要である．

索引用語：1b型高ウイルス量C型慢性肝炎　PEG IFNα-2b/リバビリン併用療法　高齢者　発癌抑制　AFP

## 緒　言

C型慢性肝炎は肝硬変や肝癌に進展する重篤な疾患である．近年，C型慢性肝炎の高齢化が顕著であり[1)]，それに伴って肝癌発生も高齢化する傾向にあり，肝癌好発年齢は60歳代になっている[2)]．一方，適切なIFN治療によりC型慢性肝炎の治療がなされ著効に持ち込めれば，肝発癌率を低下させることが示されている[3)]．C型肝炎のゲノタイプについていえば，日本においては70%が1b型で，残りの30%が2a，2b型である．1b型のうち，70%が高ウイルス量の患者である[4)]．こうした1b型高ウイルス量の患者に対して，従来のIFN単独療法は10%以下の低い著効率しかもたらさなかった[5)]．

IFN治療の進歩，すなわちPEG IFNα-2b/リバビリン治療（併用療法）は1b型高ウイルス量患者においても50～60%の高い著効率をもたらしている[6)7)]．ただ，1b型高ウイルス量患者に対するこの併用療法においても，インスリン抵抗性[8)9)]，肝脂肪化[10)]，肝線維化の進んだ症例，肥満例，女性，高齢者などで著効率が低い傾向にある[8)]．しかし，1b型高ウイルス量高齢者C型慢性肝炎に対する併用療法に関してその著効率，著効に関する因子，及び発癌抑制の検討は少ない．

この併用療法のもう一つの問題点はPEG IFNα-2b投与による食欲不振，全身倦怠，血球減少の副作用に加えて，リバビリン投与による貧血などの副作用が顕著なこと，とりわけ高齢者においてその副作用のために治療の継続を困難にしていることである[11)～13)]．ただ，その中断時期，中断率，中断理由の検討は少ない．そこで，1b型高ウイルス量高齢者C型慢性肝炎に対する併用療法の現状を把握する目的で65歳以上の高齢者の症例を65歳未満の症例と比較した．

1）神戸朝日病院消化器科
2）神戸朝日病院薬剤部
3）神戸朝日病院地域医療連携室
4）神戸大学大学院微生物学
5）兵庫県立がんセンター外科
6）順心病院外科
7）近畿大学消化器内科
8）神戸大学大学院遺伝病統御学分野
*Corresponding author: asahi-hp@arion.ocn.ne.jp

＜受付日2007年8月3日＞＜採択日2008年2月28日＞

Table 1　Host-dependent, virus related profile in the Elderly and Non-Elderly group

| group | Elderly group | Non-Elderly group | *P*-value |
|---|---|---|---|
| Gender (M/F) | 10/6 | 23/17 | 0.73 |
| IFN treatment (retrial/naive) | 4/9 | 22/17 | 0.11 |
| HCV RNA level (KIU/mL) | 2069±1380 | 1727±1581 | 0.35 |
| HCV core antigen (fmol/L) | 11058±13549 | 7256±7634 | 0.10 |
| AST (IU/L) | 40.4±19.4 | 46.3±33.7 | 0.96 |
| ALT (IU/L) | 39.8±19.9 | 52.9±38.0 | 0.39 |
| Hb (g/dL) | 13.7±1.39 | 13.9±1.65 | 0.93 |
| WBC (/μL) | 53.0±21.0 | 45.8±11.9 | 0.28 |
| PLT ($10^4$/μL) | 16.5±6.45 | 15.6±4.93 | 0.77 |
| AFP (ng/mL) | 10.1±9.55 | 12.0±29.9 | 0.30 |
| HOMA-IR | 11.5±17.5 | 5.70±5.63 | 0.20 |
| BMI (%) | 23.5±4.21 | 22.3±3.71 | 0.31 |
| F0, 1/F2, 3 | 3/9 | 20/12 | 0.03 |

## 対象と方法

対象は，当院でPEG IFNα-2b/リバビリンの併用療法を48週行ない，2007年4月までに治療を終了した1b型高ウイルス量（HCV RNA定量ハイレンジ法で100 KIU/ml以上）C型慢性肝炎患者75名である．65歳以上の症例（以下，高齢群）23名（65歳～75歳　平均69.4歳　男性14名，女性9名），65歳未満の症例（以下，非高齢群）52名（28歳～64歳　平均53.5歳　男性33名，女性19名）である．両群間の患者背景をTable 1に記した．まず両群の著効率を検討した．著効とは，併用療法終了後6カ月においてもHCV-RNA陰性症例と定義した．又，全症例についてウイルスダイナミックスのマーカーとしてのHCVコア抗原減少率（測定時HCVコア抗原量/併用療法投与前　HCVコア抗原量）を24時間後，1週，2週，4週後に測定した．

HCVコア抗原量はIRMA法（fmol/L）（Ortho Clinical Diagnostics, Tokyo, Japan）で測定した．IFN誘導蛋白としての2-5AS（オリゴアデニレートシンゼターゼ）の応答率（測定時2-5AS量/併用療法投与前2-5AS量）を2，8，12，24，48週で測定した．2-5ASはRIA法（pmol/dL）（Eiken Immunochemical Laboratory, Tokyo, Japan）で測定した．治療前後のAFP値（ng/ml）を検討した．血球減少率はHb，白血球，血小板の減少率を4週から48週まで4週毎に測定した．治療を完遂した例について，PEG IFNα-2b及びリバビリンの減量症例数を検討した．治療を中断した症例について，両群とも中断症例数と中断した時期，中断の理由を検討した．

## 結　果

患者背景で高齢群で線維化が進行していたが（P＝0.03），それ以外の初回治療例の割合，男女比，HCV RNA量，HCVコア抗原量，AST値，ALT値，Hb値，白血球数，血小板数，AFP値，HOMA-IR，BMIでは両群間に差はなかった（Table 1）．著効率では，高齢群では37.5％（6/16），非高齢群では50％（20/40）で，統計学的に有意差はみられなかった（Fig. 1）．又，高齢群では男性の著効率は50％（3/6），女性は50％（3/6），性差はなく，非高齢群でも男性の著効率は65％（13/20）で女性は35％（7/20）で性差はなかった（P＝0.058）．

開始時と24時間後，1，2，4週後におけるコア抗原減少率においては，24時間後において高齢群でやや低い傾向はあったが（P＝0.069），1，2，4週間後では有意差はみられなかった（Fig 2）．2-5AS応答率のデーターでは，いずれの時点でも両群間に有意差は認めなかった（Fig. 3）．

又，高齢群は著効例（AFP3.97±1.84 ng/ml）が非著効例（14.1±10.6 ng/ml）に比して開始時のAFP値が有意に低値であった（P＜0.01）（Fig. 4）．非高齢群では開始時のAFP値は著効例（5.27±4.08 ng/ml）と非著効例（18.7±41.6 ng/ml）との間に有意差はなかった（P＝0.125），高齢群ではAFP値は治療前後で有意な低下がみられ（開始時10.1±9.55 ng/ml，終了時5.18±4.52 ng/ml）（P＜0.05），著効例（開始時3.97±1.84 ng/ml，

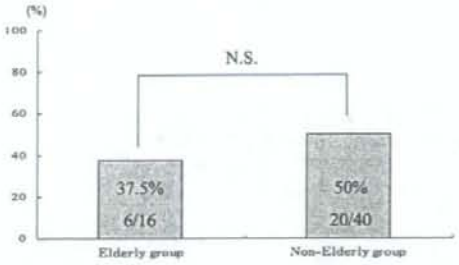


**Fig. 1** The rate of sustained virologic response

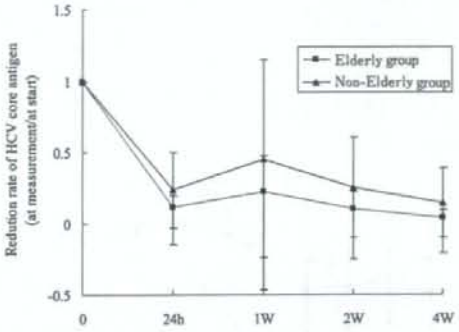


**Fig. 2** The reduction rate of HCV core antigen

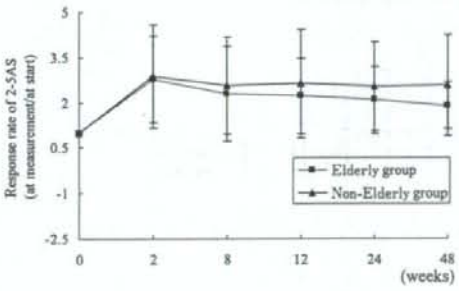


**Fig. 3** The response rate of 2-5AS

終了時2.90±1.06 ng/ml) のみならず (P<0.05)，非著効例 (開始時 14.1±10.6 ng/ml，終了時 6.11±5.33 ng/ml) においてもみられた (P<0.05) (Fig. 4，Fig. 5)．非高齢群は開始時 AFP 値 12.0±29.9 ng/ml であったが，終了時 10.5±24.7 ng/ml で治療前後で有意差はなかった

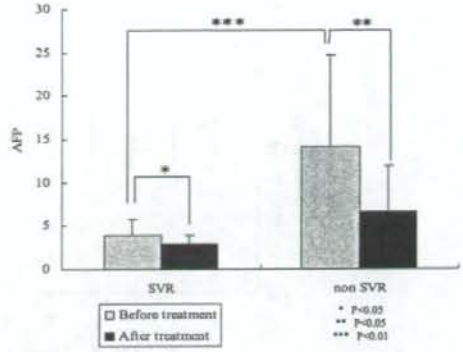


**Fig. 4** The change of AFP values in the Elderly group

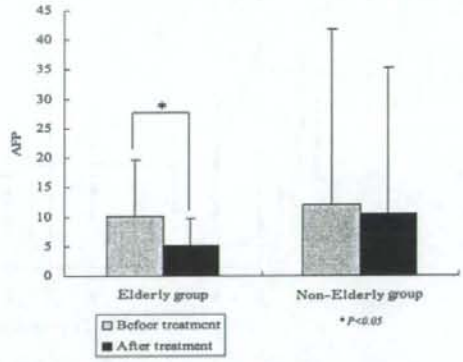


**Fig. 5** The change of AFP values in the Elderly and Non-Elderly group

(P=0.052) (Fig. 5)．治療開始時から4週間毎のHb量の減少率では，20週で高齢群(高齢群減少率(0.72±0.077))は，非高齢群 (非高齢群減少率 (0.78±0.093)) と比較して有意に低下していたが (P=0.033)，その他のいずれの時点でも両群間において差はなかった(Fig 6)．白血球数の減少率では，いずれの時点でも両群間に有意差はみられなかった(Fig. 7)．血小板数の減少率についても，いずれの時点でも両群間で有意差はみられなかった (Fig. 8)．

治療を完遂した症例で，PEG IFNα-2b を減量した症例は全体で4例あり，高齢16例中1例 (6.2%)，非高齢群40例中3例 (7.5%) で両群間に差はなかった．

治療を完遂した症例で，リバビリンを減量した症例

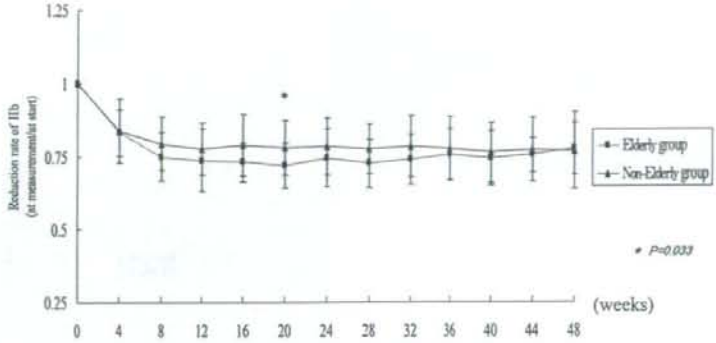


**Fig. 6** The reduction rate of hemoglobin

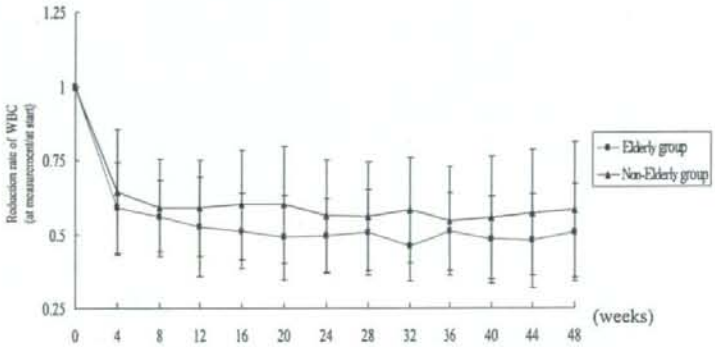


**Fig. 7** The reduction rate of white blood cells

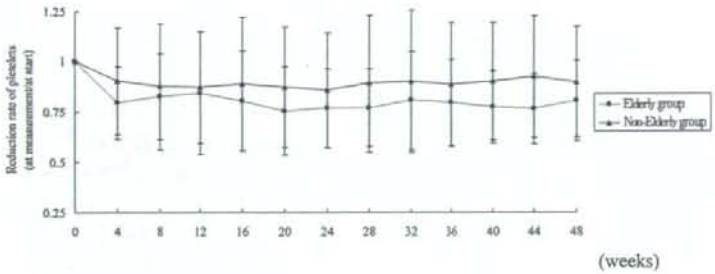


**Fig. 8** The reduction rate of platelets

は全体で13例あり，高齢群16例中3例（18.8%），非高齢群40例中10例(25%)で両群間に差はなかった．治療を中断した19例について検討したところ，高齢群は23例中7例(30.4%)，非高齢群は52例中12例(23.1%)で，両群間で中断率に差はみられなかった．治療を中断した理由として，高齢群は4週以内に4例57%（4/7)で，血小板数減少1例，発熱1例，全身倦怠2例，8週以内に全身倦怠1例で，20週以内に自己中断1例

**Table 2** The cases of discontinuation

| | | |
|---|---|---|
| Elderly group | | |
| 4 weeks after therapy | 4 cases | thrombocytopenia (1 case) |
| | | high fever (1 case) |
| | | general fatigue (2 cases) |
| 8 weeks after therapy | 1 case | general fatigue |
| 20 weeks after therapy | 1 case | self-discontinuation |
| 45 weeks after therapy | 1 case | interstitial pneumonia |
| Non-Elderly group | | |
| 4 weeks after therapy | 5 cases | depression (1 case) |
| | | self-discontinuation (2 cases) |
| | | general fatigue (1 case) |
| | | another disease (1 case) |
| 8 weeks after therapy | 3 cases | another disease (1 case) |
| | | self-discontinuation (2 cases) |
| 20 weeks after therapy | 2 cases | self-discontinuation |
| 24 weeks after therapy | 2 cases | another disease (1 case) |
| | | interstitial pneumonia (1 case) |

で，45週に間質性肺炎1例であった．非高齢群は4週以内に5例41.7%(5/12)で，うつ症状が1例，自己中断が2例，全身倦怠が1例，他疾患治療が1例，8週以内に3例で，他疾患治療1例，自己中断2例，20週以内に自己中断が2例，24週以内に2例で，他疾患治療1例，間質性肺炎1例であった（Table 2）．

## 考　察

患者背景で線維化が高齢群に進行していた．初回治療例の割合，男女比，HCV RNA量，HCVコア抗原量，AST値，ALT値，Hb値，白血球数，血小板数，AFP値，HOMA-IR，BMI，に両群間に差はなかった．併用療法のこれまでの治療成績をみると著効率に与える宿主因子として肝病理組織の脂肪化，線維化，閉経後の女性などの因子とともに高齢化が挙げられている[10]．しかし，我々の検討では著効率は高齢群と非高齢群との間に統計的には有意差はみられなかった．その原因として，今回の我々の検討では症例数が少なく，small groupによる検討であったことが関係している可能性がある．

又，高齢群と非高齢群との間に著効率に有意差がみられなかった要因としてウイルスダイナミックスのマーカー[14]としてのHCV抗原減少率[14~16]とIFN誘導蛋白の動態としての2-5AS応答率[15][17]とが両群間で同様な傾向を示し有意差を示さなかったことが挙げられる．C型慢性肝炎のIFN治療においてウイルスダイナミックスについてはIFNが直接肝細胞に働いて抗ウイルス蛋白を合成し，その作用により24時間以内でウイルスが急速に減少する投与後24時間までの第1期と，次いで上記の直接の抗ウイルス作用と細胞障害性Tリンパ球の働きによってC型肝炎ウイルス感染肝細胞が排除される投与後24時間から2週間までの第2期に分けられる[18][20][21]．1期，2期のいずれの時期においても高齢群と非高齢群においてウイルスダイナミックスすなわちHCV抗原減少率において差はみられなかった[19]．

2-5ASはIFNを投与された細胞で発見されたウイルスの増殖に必要な蛋白の阻害酵素であり，IFNの抗ウイルス活性と関係していることが確認された[22][23]．その後，2-5ASの上昇がIFN治療効果の予測に有用であることが示された[24~26]．ただ，今回の我々の検討では，2-5AS応答率はいずれの時点でも高齢群と非高齢群において差はみられなかった．

開始前のAFP値については高齢群と非高齢群の間に差はなかった．高齢群では治療前後でAFP値の低下がみられた．しかもそれは著効例のみならず，非著効例においてもみられた．非高齢群では治療前後にAFP値の有意の低下はみられていない．高齢群にみられた併用療法による治療前後のAFP値の低下がすべてIFNによる発癌抑制作用[27]によるものかどうかはにわかには断じがたい．AFP値低下が肝機能改善や線維化改善による可能性もあるからである．しかし，高齢群において併用療法の治療前後にみられたAFP値の低下は発癌抑制を何らかの形で反映していると考えてよいと思われる．それは60歳以上1b型高ウイルス量C型慢性肝炎患者の高齢者を対象としたIFN少量長期療法でAFP値が低下した症例からは発癌した症例がなかったという野村らの報告によっても支持される[20]．従って発癌抑制のためには高齢群において著効に至らなくても併用療法の完遂が重要である．又，高齢群における著効例は開始時のAFP値が非著効例に比較して有意に低値であった．芥田らは併用療法において開始前のAFP値が治療効果予測因子となること，その理由としてAFP値高値が線維化の進展を反映しているとしている[28]．今回我々の検討でも高齢群においては芥田らの報告と合致した．非高齢群では著効例と非著効例との間に開始時のAFP値に有意差はなかった．その理由は不明であるが，開始時AFP値が高齢群での治療効果予測因子の一つになることは重要な所見と考える．

我々の検討では患者背景として，高齢群はHb 13.7 g/dl，血小板16.5万/μl，白血球5300/μlであり，非高齢群はHb 13.9 g/dl，血小板15.6万/μl，白血球4580/μlで，高齢群と非高齢群では差はなかった．我々の今回の検討においては，併用療法後のHb，白血球，血小板などの血球の減少は20週目のHbが高齢群で有意に低下した以外，いずれの時点でも両群間に差はなかった．

治療を完遂した症例について，PEG IFNα-2bとリバビリンの減量率は両群間に差はなかった．このことも又，両群の著効率に差がなかった一つの要因として挙げられる．逆にいえば，高齢者のIFNとリバビリンの減量率を非高齢者と同様に抑えることができるなら，高齢群の著効率を非高齢群と同様に引き上げることができる．

中断症例についてみると，高齢群30.4％（7/23），非高齢群23.1％（12/52）と両群間に差はなかったが，その内容については差がみられた．すなわち高齢群においては4週目までは血小板数減少1例，発熱1例，全身倦怠2例で，8週目には全身倦怠1例，20週目に自己中断1例，45週目に間質性肺炎1例であった．非高齢群においては，4週以内5例で，その内容はうつ症状1例，自己中断2例，全身倦怠1例，他疾患治療1例であった．8週目までは3例で，他疾患治療1例，自己中断2例，20週目までは自己中断2例，24週目までは他疾患治療1例，間質性肺炎1例であった．特徴的なことは，65歳以上の高齢群で，開始後8週という早い時期に全身倦怠を訴えて中断した症例が中断症例5例中3例あったことである．非高齢群では，全身倦怠で中断した症例は中断症例10例中1例のみであった．高齢群の全身倦怠がリバビリンによる貧血によるものか，IFN投与による全身倦怠なのかは明らかでない．

1b型高ウイルス量高齢者C型慢性肝炎において併用療法が著効例のみならず，非著効例においても発癌抑制効果がみられたことは重要であり，治療の完遂こそが重要である．従って日常診療に従事する臨床医にあっては，高齢者の中断対策，とりわけ治療早期にみられる全身倦怠に対してきめ細かい対応が要求されている．そのことが1b型高ウイルス量高齢者C型慢性肝炎のIFN治療成績の向上及び発癌抑制につながるものと考えられる．

謝辞：本論文作成にあたり，御協力頂きました神戸朝日病院文書課・宮内　美奈子氏，川村　佳子氏，同薬剤部・笹瀬典子氏，神戸薬科大学病態生化学研究室・大山　紘一郎氏に感謝致します．

## 文　献

1) 戸川三省，山田剛太郎．高齢者C型慢性肝疾患へのインターフェロン治療．肝胆膵　2002；45：1033—1038
2) Hamada H, Yatsuhashi H, Yano K, et al. Impact of aging on the development of hepatocellular carcinoma in patients with posttransfusion chronic hepatitis C. Cancer 2002; 95 (2): 331—339
3) Yoshida H, Shiratori Y, Moriyama M, et al. Interferon therapy reduces the risk for hepatocellular carcinoma: National surveillance program of cirrhostic and noncirrhotic patients with chronic hepatitis C in Japan. Ann Intern Med 1999; 131: 174—181
4) Yoshizawa H. Trends of hepatitis virus carriers. Hepatol Res 2002; 24: S28—39

5) Nomura H, Tanimoto H, Kajiwara E, et al. Factors contributing to ribavirin-induced anemia. J Gastroen Hepatol 2004; 19: 1312—1317
6) Manns MP, McHutchison JG, Gordon SC, et al. Peginterferon alfa-2b plus ribavirin compared with interferon alfa-2b plus ribavirin for initial treatment of chronic hepatitis C: a randomised trial. Lancet 2001; 358: 958—965
7) Fried MW, Shiffman ML, Reddy KR, et al. Peginterferon alfa-2a plus ribavirin for chronic hepatitis C virus infection. N Engl J Med 2002; 347: 975—982
8) Romero-Gomez M, Del MV, Andrade RJ, et al. Insulin resistance impairs sustained response rate to peginterferon plus ribavirin in chronic hepatitis C patients. Gastroenterology 2005; 128 (3): 636—641
9) D'Souza R, Sabin CA, Foster GR. Insulin resistance plays a significant role in liver fibrosis in chronic hepatitis C and in the response to antiviral therapy. Am J Gastroenterol 2005; 100 (7): 1509—1515
10) Yaginuma R, Ikejima K, Okumura K, et al. Hepatic steatosis is a predictor of poor response to interferon alpha-2b and ribavirin combination therapy in Japanese patients with chronic hepatitis C. Hepatol Res 2006; 35: 19—25
11) Nomura H, Tanimoto H, Kajiwara E, et al. Factors contributing to ribavirin-induced anemia. J Gastroen Hepatol 2004; 19: 1312—1317
12) Hiramatsu N, Oze T, Tsuda N, et al. Should aged patients with chronic hepatitis C be treated with interferon and ribavirin combination therapy? Hepatol Res 2006; 35: 185—189
13) Okanoue T, Sakamoto S, Itoh Y, et al. Side effects of high-dose interferon therapy for chronic hepatitis C. J Hepatol 1996; 25: 283—291
14) Buti M, Mendez C, Schaper M, et al. Hepatitis C virus Core Antigen as a predictor of non-response in genotype 1 chronic hepatitis C patients treated with peginterferon α-2b plus ribavirin. J Hepatol 2004; 40: 527—532
15) Veillon P, Payan C, Pcchio G, et al. Comparative evaluation of the total hepatitis C virus core antigen, branched-DNA, and amplicor monitor assays in determining viremia for patients with chronic hepatitis C during interferon plus ribavirin combination therapy. J Clin Microbiol 2003; 41: 3212—3220
16) Zanetti AR, Romano L, Brunetto M, et al. Total HCV core antigen assay: a new marker of hepatitis C viremia for monitoring the progress of therapy. J Med Virol 2003; 70: 27—30
17) Kim KI, Kim SR, Sasase N, et al. 2′-, 5′-Oligoadenylate synthetase response ratio predicting virological response to PEG-interferon-α 2b plus ribavirin therapy in patients with chronic hepatitis C. J Clin Pharm Ther 2006; 31: 441—446
18) Yasui K, Okanoue T, Murakami Y, et al. Dynamics of hepatitis C viremia Following interferon-alpha administration. J Infect Dis 1998; 177: 1475—1479
19) Neumann AU, Lam NP, Dahari H, et al. Hepatitis C viral dynamics in vivo and the antiviral efficacy of interferon-alpha therapy. Science 1998; 282: 103—107
20) Anonymous. National Institutes of Health Consensus Development Conference Statement: Management of hepatitis C. Hepatology 2002; 36: S3
21) Anonymous. Consensus conference. Treatment of Hepatitis C. Agence Nationale d'Accreditation et d'Evaluation en Sante (ANAES). Gastroen Clin Biol 2002; 26: B303
22) Schmidt A, Zilberstein A, Shulman L, et al. Interferon action: isolation of nuclease F, a translation inhibitor activated by interferon-induced (2′, 5′) oligoisoadenylate. FEBS Lett 1978; 95: 257
23) Nilsen TW, McCandless S, Baglioni C. 2′, 5′-oligo (A)-activated endonuclease in NIH 3T3 mouse cells chronically infected with Moloney murine leukemia virus. Virology 1982; 122: 498
24) Karino Y, Hige S, Matsushima M, et al. Significance of 2′, 5′-oligoadenylate synthetase activity and HCV genotype in IFN therapy for type C chronic hepatitis. Hokkaido Igaku Zasshi 1994; 69: 1354
25) Toda K, Kumagai N, Iwabuchi N, et al. 2-5AS activity in serum and peripheral blood mononuclear cells for chronic active hepatitis C and the relationship to clinical outcome of interferon therapy. Jpn J Clin Immunol 1997; 20: 428
26) Tong WB, Zhang CY, Feng BF, et al. Establishment of a nonradioactive assay for 2′, 5′ oligoadenylate synthetase and its application in chronic hepatitis C patients receiving interferon-alpha. World J Gastroenterol 1998; 4: 70
27) Yano H, Yanai Y, Momosaki S, et al. Growth inhibi-

tory effects of interferon-α subtypes vary according to human liver cancer cell lines. J Gastroenterol Hepatol 2006; 21: 1720—1725
28) Nomura H, Kashiwagi Y, Hirano R, et al. Efficacy of low dose long-term interferon monotherapy in aged patients with chronic hepatitis C genotype 1 and its relation to alpha-fetoprotein: A Pilot study. Hepatol Res 2007; 37: 490—497
29) Akuta N, Suzuki F, Kawamura Y, et al. Predictors of viral kinetics to peginterferon plus rivavirin combination therapy in Japanese patients infected with hepatitis C virus genotype 1b. J Med Virol 2007; 79 (11): 1686—1695

# Pegylated interferon α-2b/ribavirin combination therapy for elderly patients with chronic hepatitis C with high viral load of HCV genotype 1b

Soo Ryang Kim[1]*, Susumu Imoto[1], Shuichi Fuki[1], Ke Ih Kim[2], Miyuki Taniguchi[3], Motoko Nagano[4], Hak Hotta[4], Ikuo Shouji[5], Yoshihiro Kanbara[5], Yoko Maekawa[6], Masatoshi Kudo[7], Yoshitake Hayashi[8]

The patients (n＝75) in this study had chronic hepatitis C with high viral loads of serum HCV-RNA genotype 1b. All the patients received a regimen of pegylated interferon α-2b plus ribavirin (PEG IFN α-2b/RBV) for 48 weeks. Comparative analysis was done by dividing these patients into two groups by age: Elderly group (over 65 years old, 23 patients) and Non-Elderly group (under 65 years old, 52 patients). The sustained viral response (SVR) rate in the Elderly (37.5%, 6/16) was not different significantly from that in the Non-Elderly (50%, 20/40). The response ratio of 2′-5′-oligoadenylate synthetase (2-5AS), the viral dynamics and the rate of discontinuation of therapy were not different between the two groups. Interestingly, however, the mean α-fetoprotein (AFP) values decreased significantly in the Elderly irrespective of SVR or non-SVR (from 10.1 ± 9.55 ng/ml before treatment to 5.18 ± 4.52 ng/ml after treatment, $P<0.05$), but did not in the Non-Elderly. It was thus suggested that Peg IFN α-2b/RBV would be useful in the prevention of HCC in elderly patients including non-SVR cases.

**Key words:** chronic hepatitis C　pegylated interferon α-2b/ribavirin combination therapy　elderly patients　prevention of hepatocarcinogenesis　AFP

*Kanzo* 2008; 49: 145—152

1) Department of Gastroenterology, Kobe Asahi Hospital
2) Department of Pharmacy, Kobe Asahi Hospital
3) Medical Information Center, Kobe Asahi Hospital
4) Division of Microbiology, Kobe University Graduate School of Medicine
5) Department of Surgery, Hyogo Cancer Center
6) Department of Surgery, Junshin Hospital
7) Department of Gastroenterology, Kinki University Medical School of Medicine
8) Division of Molecular Medicine & Medical Genetics, Kobe University Graduate School of Medicine
*Corresponding author: asahi-hp@arion.ocn.ne.jp

# Morphological identification of hepatitis C virus E1 and E2 envelope glycoproteins on the virion surface using immunogold electron microscopy

MASAHIKO KAITO[1], SHOZO WATANABE[2], HIDEAKI TANAKA[1], NAOKI FUJITA[1], MASAYOSHI KONISHI[1], MOTOH IWASA[1], YOSHINAO KOBAYASHI[1], ESTEBAN CESAR GABAZZA[1], YUKIHIKO ADACHI[1], KYOKO TSUKIYAMA-KOHARA[3] and MICHINORI KOHARA[3]

[1]Department of Gastroenterology and Hepatology, Division of Clinical Medicine and Biomedical Science, Institute of Medical Science, Mie University Graduate School of Medicine, 2-174 Edobashi, [2]Health Administration Center, Mie University, 1577 Kurimamachiya-cho, Tsu, Mie 514-8507; [3]Department of Microbiology of Cell Biology, Tokyo Metropolitan Institute of Medical Science, 3-18-22, Honkomagome, Bunkyo-ku, Tokyo 113-8613, Japan

Received April 24, 2006; Accepted June 20, 2006

**Abstract.** It is known that hepatitis C virus (HCV) particles are spherical, 55-65 nm particles with fine surface projections of about 6 nm in length and with a 30-35 nm inner core. We have reported that free HCV particles labeled with gold particles specific to the HCV E1 glycoprotein are located in 1.14-1.16 g/ml fractions from plasma samples with high HCV RNA titers after sucrose density gradient centrifugation. However, the morphology of the HCV E2 glycoprotein on the virion has not yet been elucidated. To visualize HCV E2 localization on the virion, we used the same plasma samples where HCV particles were clearly shown. An indirect immunogold electron microscopic study was carried out using monoclonal and polyclonal anti-HCV E2 antibodies. HCV-like particles specifically reacted with the anti-HCV E2 antibodies. Moreover, to evaluate the localization of the HCV E1 and E2 glycoproteins on the virion surface, an immunogold electron microscopic study using double labeling with anti-HCV E1 antibodies and anti-HCV E2 antibodies was also performed. These particles also specifically reacted with both anti-E1 and E2 antibodies. This is the first report showing the presence of both HCV E1 and E2 glycoproteins on HCV virion surface in human plasma samples.

*Correspondence to*: Dr Masahiko Kaito, Department of Gastroenterology and Hepatology, Division of Clinical Medicine and Biomedical Science, Institute of Medical Science, Mie University Graduate School of Medicine, 2-174 Edobashi, Tsu, Mie 514-8507, Japan
E-mail: kaitoma@clin.medic.mie-u.ac.jp

*Abbreviations*: HCV, hepatitis C virus; ALT, alanine aminotransferase; PCR, polymerase chain reaction; EM, electron microscopy; RVV, recombinant vaccinia virus; ELISA, enzyme-linked immunosorbent assay; IFA, indirect immunofluorescence assay; WB, Western blot analysis; BSA, bovine serum albumin; Huh7, a human hepatoma cell line

*Key words:* hepatitis C virus, E1, E2, electron microscopy, virion

## Introduction

Hepatitis C virus (HCV) is the main causative agent of non-A non-B hepatitis. It is estimated that 170 million individuals are infected with HCV worldwide (1). HCV is a hepatotropic, enveloped RNA virus that belongs to the genus *Hepacivirus* of the *Flaviviridae* family (2), and it is the leading cause of acute hepatitis, chronic hepatitis, liver cirrhosis and hepatocellular carcinoma in humans (1,3-6). The HCV genome is a positive-stranded RNA of 9.6 kb containing a single open reading frame and two untranslated regions (7-9). It encodes a polyprotein of 3010 amino acids, which is cleaved into single proteins by a host signal peptidase in the structural region and by HCV-encoded proteases in the nonstructural region. Structural components include the capsid protein and the envelope glycoproteins E1 and E2. The nonstructural components include NS2, NS3, NS4A, NS4B, NS5A and NS5B. The NS2, NS3, and NS 4A proteins function as proteases, the NS3 protein as helicase, and the NS5B protein as RNA-dependent RNA polymerase (1).

HCV E1 and E2 glycoproteins are possible virion envelope glycoproteins, and their molecular weights are 35 and 70 kDa, respectively (10,11). The comparison of HCV genome structure with flaviviruses suggests that HCV E1 (gp35) and E2 (gp70) glycoproteins interact forming heterodimer complexes as the basic subunit of the HCV virion envelope (11,12). However, this has not been confirmed morphologically. We previously demonstrated that HCV particles are spherical, 55-65 nm particles with fine surface projections of about 6 nm in length and with a 30-35 nm inner core by immunoelectron microscopic study using anti-HCV E1 antibodies (13-17). Free HCV particles were found in 1.14-1.16 g/ml fractions after sucrose density gradient

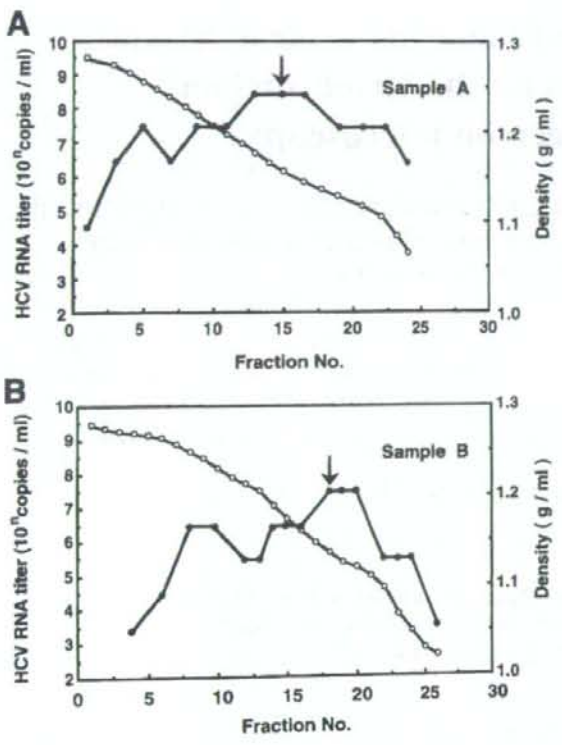


Figure 1. HCV-RNA titers in fractions from samples A and B obtained by sucrose density gradient centrifugation. HCV RNA titers (●) and buoyant densities (○) are shown: (A) sample A, (B) sample B. Arrows indicate the fractions (1.14-1.16 g/ml) in which HCV particles were successfully detected by immunogold EM using rabbit anti-HCV E1 polyclonal antibody (RR2).

centrifugation. However, the morphology of the HCV E2 glycoprotein on the virion has not as yet been elucidated.

In this study, we carried out indirect immunogold electron microscopy (EM) in order to evaluate the localization of the HCV E1 and E2 glycoproteins on the surface of HCV particles isolated from plasma samples with high HCV RNA titers.

## Materials and methods

*Virus samples*. Plasma samples where HCV particles were clearly shown, were used to determine the HCV E2 localization on HCV particles. HCV particle isolation and indirect immunogold EM were performed as previously described (13). In brief, virus samples from HCV RNA-rich plasma sample A [alanine aminotransferase (ALT): $10^3$ IU/l, HCV RNA: genotype 1b (18), $4x10^7$ copies/ml] and B (ALT: $10^9$ IU/l, genotype 1b, $5x10^7$ copies/ml), and anti-HCV-negative plasma sample C (ALT: 121 IU/l) and D (ALT: 87 IU/l) were prepared as follows: 100 ml of plasma were centrifuged at 75000 g for 6 h at 4°C and the suspension of the pellet was centrifuged again at 150000 g for 2.5 h at 4°C. A 1000-fold concentrated suspension of the sample was layered on a 20-60% (w/w) continuous sucrose density gradient in TNE buffer (50 mM Tris-HCl, pH 7.5, 100 mM NaCl, 1 mM EDTA), and centrifuged at 100000 g for 16 h at 4°C. Sucrose fractions (500 μl) were collected from the tube bottom, and the sucrose densities were measured with an Abbé refractometer. The distribution of HCV RNA titers was determined using competitive polymerase chain reaction (PCR) (19,20). HCV RNA titers in fractions from samples A and B obtained by sucrose density gradient centrifugation were previously described (13,17). The density at which the highest HCV RNA titers (sample A, $5x10^8$ copies/ml; sample B, $5x10^7$ copies/ml) were found was 1.14-1.17 g/ml for sample A and 1.12-1.14 g/ml for sample B (Fig. 1). For preparing a 1000-fold concentrated virus sample, each sucrose fraction was diluted in 12 ml of PBS (pH 7.4), and spun down at 150000 g for 2.5 h at 4°C. The pellets were then suspended in 100 μl of PBS. The fractions (1.14-1.16 g/ml) in which HCV particles were successfully detected by immunogold EM using rabbit anti-HCV E1 polyclonal antibody (13) were used for virus sampling.

*Rabbit polyclonal and mouse monoclonal antibodies to HCV E2 glycoprotein*. The rabbit polyclonal anti-HCV E2 antibody (RR6) was prepared and characterized as follows. The putative E2 gene of HCV genotype 1b (nucleotide position 1068-2430) (8,10) was cloned under the control of the ATL-P7.5 hybrid promoter of the vaccinia virus vector pSFB4 (21), and allowed to recombine with the Liter strain of vaccinia virus to give a vector recombinant vaccinia virus (RVV). Rabbits were infected intradermally with $10^8$ p.f.u. of RVV and 2 months later were boosted twice with the purified putative E2 glycoprotein. Putative HCV E2 glycoprotein was expressed by RVV and purified by lentil lectin column chromatography and affinity chromatography using an anti-E2 monoclonal antibody. Mouse monoclonal antibodies (747, 843, 1518, 1671, and 1864) against the putative HCV [genotype 1b (17)] E2 glycoprotein were prepared by immunization of mice with purified recombinant E2 glycoprotein (gp70) expressed by RVV. The antibody RR6 and the monoclonal antibodies were screened by enzyme-linked immunosorbent assay (ELISA) using synthetic peptides and purified recombinant protein, indirect immunofluorescence assay (IFA) using RVV- and baculovirus-infected (22) rabbit kidney cells, and Western blot analysis (WB) using purified E2 protein region of HCV genotype 1b as antigens (8). The epitope of monoclonal antibodies was mapped using residues of 20 synthetic peptides whose adjacent peptides overlap by 10 amino acids corresponding to the amino acid sequence reported by Kato *et al* (7). The characteristics of anti-HCV E2 antibodies used as the primary antibody of the indirect immunogold reaction were determined (Table I). The antibody RR6 and the monoclonal antibodies reacted specifically with the putative HCV E2 glycoprotein, but it did not react with the putative HCV core, E1, or NS2 proteins. Specificity was determined by using primary antibodies from pre-immune normal rabbit serum, serum from a rabbit infected with the Lister strain of vaccinia virus and monoclonal antibody specific to human blood type A antigen as negative controls, or by omitting the use of the primary antibody.

*Rabbit polyclonal and mouse monoclonal antibodies to HCV E1 glycoprotein*. The rabbit polyclonal antibody (RR2) and